**Reference Code:** hess-2018-393

**Title:** Spatially dependent flood probabilities to support the design of civil infrastructure systems

**Corresponding Author:** Phuong Dong Le (The University of Adelaide)

**Contributing Authors:** Michael Leonard and Seth Westra

## Response to the Reviewer

*The authors have significantly modified and improved the manuscript, taking into account the reviewers' comments. However I still think that the manuscript needs to be improved on three main points before publication (see below for the details and additional comments):*

**Response:** Thank you for your comments. We respond in detail below (your comments in italic font and our responses in normal font).

**Major comment #1:**

*The presentation of the inverted Brown-Resnick model is still unclear (Sections 4.2 to 4.4). I think it will hardly be understandable by the readers of HESS.*

**Response**: The focus of this paper is on application to a design problem, therefore we have focused on explaining key aspects of the application. Rather than seek to repeat or elaborate background theory and definitions of the Brown-Resnick model, we have now simplified the presentation and point readers to papers that give the clearest presentation of the Brown-Resnick model. As a result, Sections 4.2 and 4.3 have been merged, with some theoretical background material and equations removed. Section 4.4 has been moved to the Appendix because it includes necessary calculations for the conditional framework, but otherwise interrupts presentation of the overall framework and application.

**Major comment #2:**

*Section 4.5 and 4.6 should be better motivated beforehand. Personally I understood these sections only when reading Sections 5.2 and 5.3. The few sentences at the beginning of Section 4 and Figure 14 are not clear enough for me to understand what are the needed mathematical ingredients.*

**Response**: Given ambiguity in explanation of the method, we have made a substantially different version of Figure 4. The new flow chart gives a clearer presentation of the key stages and how they are interlinked. The items in the flowchart now mirror the presentation of material in Sections 5.2 and 5.3 to improve consistency of presentation in Section 4. Excerpt text from Line 197-209:

> This section describes the method used to estimate the conditional and joint probabilities of streamflow for civil infrastructure systems based on rainfall extremes, with the sequence of steps illustrated in Fig. 4. The overall aim is to estimate rainfall exceedance probabilities and corresponding flow estimates that account for dependence across multiple catchments. The generalized Pareto distribution (GPD) is used as the marginal distribution to fit to observed rainfall for all durations at each location (Section 4.1). An extremal dependence model is required to evaluate conditional and joint probabilities. Here, an inverted max-stable process is used with dependence not only in space but also in duration (Section 4.2). The fitted model is evaluated in a range of contexts, including the construction of joint and conditional return level maps. The derivation of areal reduction factors and joint rainfall estimates are made with the assistance of simulations based on the fitted model (Section 4.3). An event-based rainfall-runoff model is employed in Section 4.4 to transform extremal design rainfalls to corresponding flows.

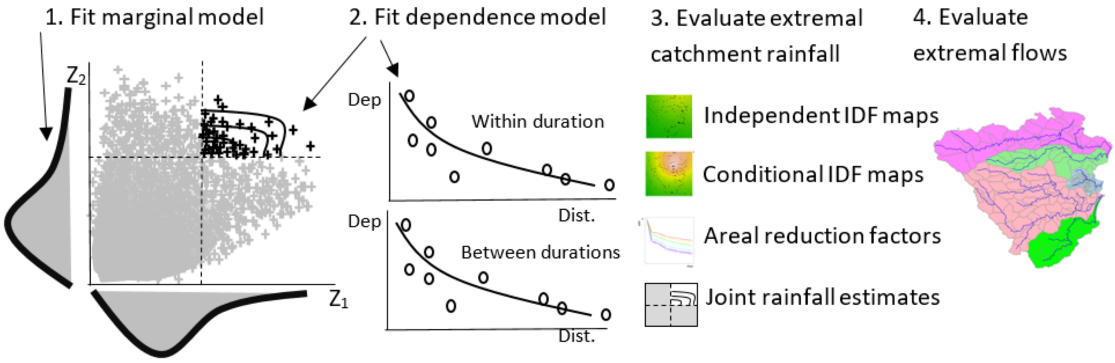


**Figure 4.** The flow chart for the overall methodology.

**Major comment #3:**

*Several equations lack consistency (see below).*

**Response**: Specific comments have been given to each point raised below. Some of the background theory has been removed for simplification. Some of the equations have been moved to an appendix to avoid interrupting overall methodology. The unit Frechet transformation has been added, the tail dependence equation has been updated.

**Minor comment #1:**

*– The title hasn't been changed (unlike written in the response to Major Comment 1). Anyway, even with « relationships », I still find the title confusing with regards to content of the article. Why not « Spatially dependent flood probabilities to support ... » ?*

**Response**: We have changed the title to "Spatially dependent flood probabilities to support the design of civil infrastructure systems"

**Minor comment #2:**

*– L 63-64 « to overcome... used » : repetition with the previous sentence*

**Response**: We have removed this sentence.

**Minor comment #3:**

*– L 138 « the lack of dependence » → the underlying independence assumption*

**Response**: We have changed this.[1]

**Minor comment #4:**

*– L 145 « preserve dependence » → account for*

**Response**: We have changed this.[2]

**Minor comment #5:**

*– L 149-150 : could you eleborate more on the difference between copula and max-stable processes ? Why did you choose to use MSP rather than copulas ?*

**Response**: We identify that it is equally possible to use copulas such as the Gaussian copula parametrised as a function of distance.[3]

[1] Line 79: The underlying independence assumption prevents these approaches from being applied to estimate conditional or joint flood risk at multiple points in a catchment or across several catchments, as would be required for a civil infrastructure system.

[2] Line 85 . This is particularly challenging given that it is not only necessary to account for dependence of rainfall across space, but also to account for dependence across storm burst durations, as different parts of the system may be vulnerable to different critical duration storm events.

[3] Line 236 This study uses an asymptotically independent model, of which there are multiple types including the Gaussian copula (Davison et al., 2012) and inverted max-stable processes (Wadsworth and Tawn, 2012).

**Minor comment #6:**

*– L 166 « spatially dependence IDF curves » → I haven't seen such curves in the manuscript*

**Response**: The manuscript presents IDF maps, but as the reviewer notes, did not present IDF curves. We have updated the title to indicate 'flood probabilities'. Within the paper we have used the phrase "*IDF estimates" and avoid reference to* IFD curves since they are not explicitly presented.

**Minor comment #7:**

*– L 262-273: This is a list of what you'll do in the next sections but we don't understand why you'll do that (what are the goals?). Please rewrite.*

**Response**: We have significantly modified Figure 4 as well as restructured Section 4 to provide greater clarity on the stages of the method and have indicated the goal of the approach.[4]

**Minor comment #8:**

*– L 269 : « to transform conditional rainfall to conditional flows » → This is confusing. I think you transform quantiles, not the absolute values.*

**Response**: The rainfall quantile from the conditional map is used for the magnitude of a design storm. The storm has an associated temporal pattern determined by the national guidelines for hydrological design (Australian Rainfall and Runoff). The absolute rainfall values of this storm are transformed by the model into a flow hydrograph.[5]

**Minor comment #9:**

*– L 271-273 « An analysis .. comparison » : Actually I don't see any comparison with the independent model (apart in Fig 10). Please remove it from Fig 4 as well.*

**Response**: Figure 4 has been updated with mention of the comparison removed.

**Minor comment #10:**

*– Figure 4: "probability of rainfall" , "conditional probability of flows", "assume 1:1 relationships for the probabilities", joint flood probability → probability of system failure (give the section number)*

**Response**: We have updated Figure 4.

---

[4] Line 199: The overall aim is to estimate rainfall exceedance probabilities and corresponding flow estimates that account for dependence across multiple catchments.

[5] Line 341: The rainfall extremes are estimated at the centroid of the catchment, and are converted to average spatial rainfall using the simulated ARFs described in Section 4.3. Design rainfall hyetographs are used to convert the rainfall magnitude to absolute values through the duration of a storm following standard design guidance in Australia (Ball et al., 2016).

**Minor comment #11:**

*– Sections 4.2 to 4.4 should be partly rewritten and reorganized.*

**Response**: We have rewritten Section 4. Figure 4 has been updated and Section 4 has been rewritten for greater consistency with the new figure. Section 4.2 has been trimmed to remove background theory of the BR model in preference for references. Section 4.2 and 4.3 have been merged and made more concise to focus on fitting the dependence model. Section 4.4 has been moved to an appendix given the detailed nature of the equations so that the method can focus more on the structure of the model.

**Minor comment #12:**

*– L 295: please specify that Z is associated to a given duration*

**Response**: The text has been updated to indicate it is for a given duration.[6]

**Minor comment #13:**

*– L 297-298 "without loss... distribution": I don't think that the reader will understand why one can assume that Z is unit Fréchet distributed. The transformation should be given.*

**Response**: The transformation equation is now provided in Appendix B.[7]

**Minor comment #14:**

*– L 305 "An example … process": Yes but the Gaussian process is another example of AI model. What is the advantage of the inverted BR model with respect to a Gaussian process?*

**Response**: It is possible to use the Gaussian copula as an asymptotic independent model. Beyond the fit of the dependence model to the data, there is no significant advantage in using one over the other. The focus of this paper is on the ability to construct conditional IDF maps and subsequent design flow estimates rather than a comparative evaluation of models.

---

[6] Line 243: For a generic continuous process $Z_i$ for a given duration and associated with a specific location $x_i$, the empirical pairwise residual tail dependence coefficient $\eta$ for each pair of locations $(x_1, x_2)$ is …

[7] Line 539: The unit Fréchet transformation is given as

$$z = \begin{cases} \left(log\left\{1 - \Phi_u\left(1 + \frac{\xi(y-u)}{\sigma_u}\right)^{-1/\xi}\right\}\right)^{-1} & y > u, \xi \neq 0 \\ -\left(log\left\{1 - \Phi_u exp\left(-\frac{y-u}{\sigma_u}\right)^{-1/\xi}\right\}\right)^{-1} & y > u, \xi = 0 \\ -\{logF(y_i)\}^{-1} & y \leq u \end{cases} \qquad (B.1)$$

where $y$ is the original marginal value and $z$ is the Fréchet transformed value and all other parameters correspond to the GPD specified in Section 4.1. For values below the threshold, $F$ is the empirical distribution function of $y$, $F(y_i) = i/(n+1)$ where $i$ is the rank of $y_i$ and $n$ is the total number of data points.

**Minor comment #15:**

*– L 308-319 "A general … margins": this is not understandable for the great majority of HESS readers. Anyway there is a lack of consistency because tin the construction (2), margins are assumed to be exponential.*

**Response**: The background theory has been removed and is treated in detail within the cited literature. The paper focuses more on the scope of model application.

**Minor comment #16:**

*– Eq (4): Again this lacks consistency: written as such, you assume that Z has uniform margins. What is y in the limit? For importantly, what does eta represent in practice? This will stay obscure for most of the readers.*

**Response**: Thank you. We have fixed the Eq (4), *y* in the limit should be z.[8]

$\eta$ is the residual dependence coefficient, which is a bivariate concept and is defined to measure residual dependence between two asymptotically independent random variables.

**Minor comment #17:**

*– L 346-360: this is a very complicated way of saying that the dependence depends not only on the distance but also on the duration. Please make it shorter and clearer. The reference to the time of concentration is confusing because it was nowhere said that you will consider for the duration the time of concentration of the basin. By the way, do you only consider that duration later?*

**Response**: The text in this section has been made more concise to omit reference to the time of concentration and say that the dependence depends on the duration.[9] The method is for any given duration, the case study application identifies relevant durations based on the time of concentration of the basins. [10]

**Minor comment #18:**

*– L 377-385: this part (at least the joint distribution) should come before in Section 4.1. Does Eq. (7): apply to any z1, z2? I guess it applies only to threshold exceedances.*

**Response**: Equations 7 to 10 have been moved to Appendix B so they do not interrupt the focus on fitting the dependence model and subsequent application. Equation B.1 in the Appendix provides the Frechet transform which indicates that Z refers to values both above the threshold and below.

---

[8] Line 243: For a generic continuous process $Z_i$ for a given duration and associated with a specific location $x_i$, the empirical pairwise residual tail dependence coefficient $\eta$ for each pair of locations $(x_1, x_2)$ is

$$\eta(x_1, x_2) = \lim_{z\to\infty} \frac{\log P\{Z_2 > z\}}{\log P\{Z_1 > z, Z_2 > z\}}. \quad (2)$$

The value of $\eta \in (0,1]$ indicates the level of extremal dependence between $Z_1$ and $Z_2$ (Coles et al., 1999), with lower values indicating lower dependence. An example of how to calculate the residual tail dependence coefficient is provided in Appendix A for a sample dataset.

[9] Line 259: The inverted max-stable process is fitted to the observations by minimizing the sum of the squared errors of the residual tail dependence coefficients. When the extreme rainfall at location $x_1$ and $x_2$ are of different durations, the dependence is less than when the extremes are of the same duration. For example, at a single location ($h$ = 0), when the duration is the same, the rainfall values are identical and have perfect dependence, but when the duration of extremes are different the values are not identical and the dependence is less. An adjustment needs to be made to the theoretical pairwise residual tail dependence coefficient function when extreme rainfalls have different durations.

[10] Line 192: … this study assumes a time of concentration of 9 hr for the Deep Creek catchment, while identical times of concentration of 36 hr are assumed for the other four catchments.

**Minor comment #19:**

*– Eq. (9): I'm confused here. (9) seems to implicitely use P(Z1>z1)=1/T1 with z1 the T1 year return level for Z1. However is that true? I though that Z1 and Z2 were threshold exceedances, whereas P(Z1>z1)=1/T1 applies if Z1 is an annual maximum, doesn't it?*

**Response**: Thank you for pointing this out. We have updated the text in the manuscript to indicate that the return periods are calculated on 36 hourly basis. Z1 and Z2 are not restricted to threshold exceedances. The derivation is shown below where the four quadrants of the bivariate space above/below respective thresholds are labelled A, B, C, D. The conditional distribution is the joint divided by the marginal B/(B+C) and where the threshold is z1 is set at *P(Z1>z1)=1/T1*.

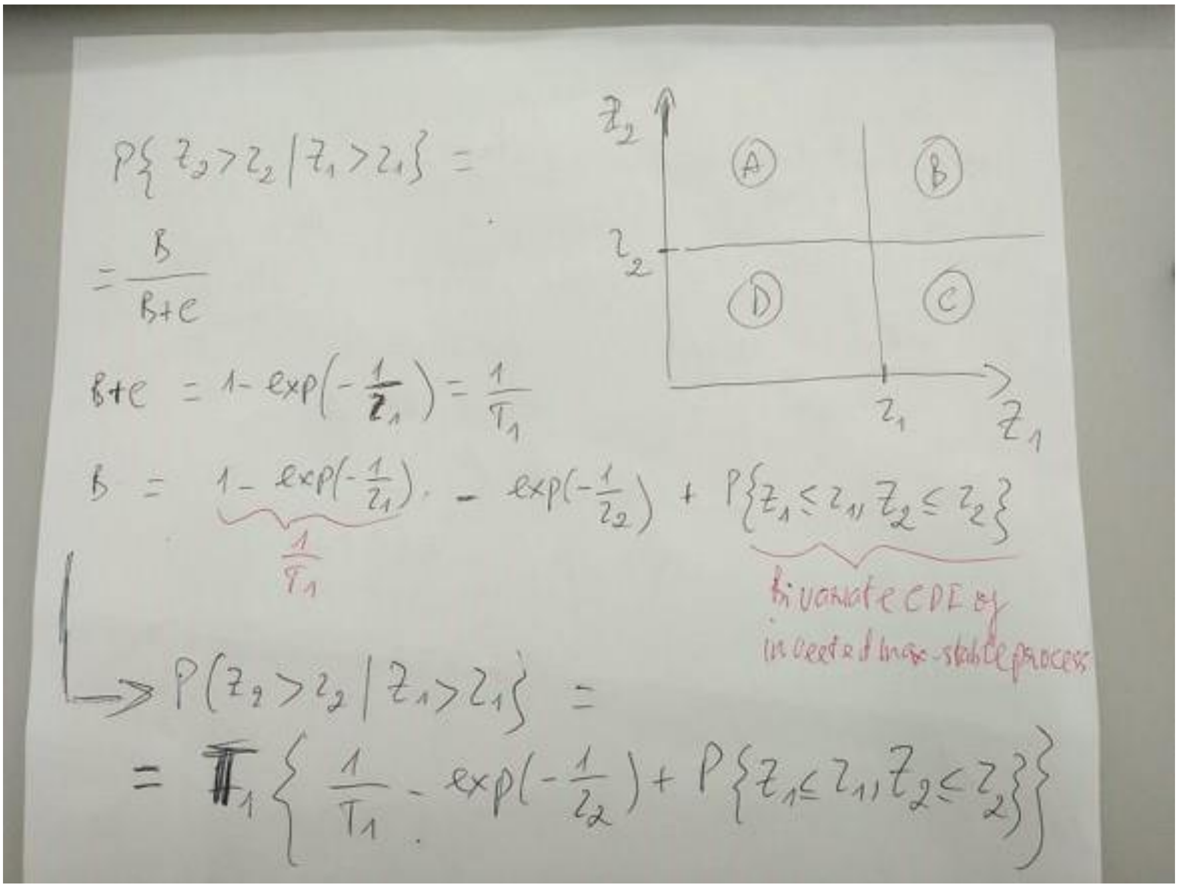


**Minor comment #20:**

*– L 428-429 "the joint probability … marginals": it could also be specified that in case of independence conditional=marginal.*

**Response**: Thank you. We have fixed this.[11]

**Minor comment #21:**

*– Eq. (10): is this useful? I don't think you use it anywhere... Anyway, if you specify this probability in the case of independence, you should also give it for the IBR process.*

---

[11] Line 573: For the case that all of events are independent, the joint probability for independent variables is broken down as the product of the marginals, and the conditional probability is equivalent to the marginal probability. When applying Eq. (B.5) for independent variables, the joint probability is therefore calculated by $P(Z_1 > z_1, \dots, Z_N > z_N) = P(Z_1 > z_1) \dots P(Z_N > z_N)$.

**Response**: Eq. (10) is useful when we calculate the joint probability for the case of independence (i.e. the blue line in Fig. 10). We have explicitly referenced it in the method section.[12]

**Minor comment #22:**

*– L 440: A better title might be "Simulation-based estimation of ARFs"*

**Response**: We have restructured Section 4 and title for this section is now 'Simulation based estimation of areal and joint rainfall'

**Minor comment #23:**

*– L 463-465 "the empirical distributions … thresholds": I don't understand how an empirical distribution can be derived using a response surface since by definition it is not parametric! And what about above the threshold?*

**Response**: We use a response surface of threshold for the case study catchments based on covariates including longitude and latitude, i.e. we spatially interpolate the threshold for ungauged sites. For the rainfall above the interpolated threshold, the generalised Pareto distribution in Eq. (1) was used. For rainfall below the interpolated threshold we use the data of the nearest gauged site and extract the empirical distribution.[13]

**Minor comment #24:**

*– L 474-475 "36 and 6 h durations": only? Other durations are shown in Fig 6...*

**Response**: Thank you. In this study, we only need ARFs for 36 and 9h durations due to the time of concentrations of sub-catchments, so we have calculated ARFs for only 36 and 9h durations.[14]

**Minor comment #25:**

*– L 475-476: "ARF are calulated": I would like to have here a clear explanation on how it is calculated because it is not clear to me.*

**Response**: This section has been rewritten.[15] The calculation of ARFs is a substantial step which is covered in detail in Le et al. (2018a). We provide a clearer explanation of the method here in brief, but rely on the reference for detailed explanation of the method. The ARFs are applied here for durations of 36 and 9 hrs.

**Minor comment #26:**

*– L 500-508: I'm a bit lost here because you seem to be able to simulate rainfall in space (see Section 4.5) so why don't you directly simulate rainfall and compute the basin accumulation rather than simulating at the centroid of the catchment and then using the ARF to transform it into a spatial accumulation? My concern is that this may introduce a bias.*

**Response**: The aim of this paper is to develop a method that preserves the traditional IDF framework, where pointwise IDF maps summarise event-magnitudes and separate steps are used to construct rainfall volumes and flow estimates. In

---

[12] Line 331: A set of 10,000 years simulated rainfall is generated from the fitted model to calculate the overall failure probability of a highway section (Eq. B.5).

[13] Line 301: For rainfall magnitudes above the threshold the generalised Pareto distribution in Eq. (1) is used, and below the threshold the empirical distribution is used. The empirical distributions at ungauged sites are derived from the nearest gauged sites and using the interpolated response surface of the GPD threshold parameter.

[14] Line 192: … this study assumes a time of concentration of 9 hr for the Deep Creek catchment, while identical times of concentration of 36 hr are assumed for the other four catchments.

[15]

other words, the ARF simulation is a once-off task, whereas application of the overall design method will vary with each context but can utilise the same ARF results.

**Minor comment #27:**

*– L 553 rainfall extremes → rainfall return levels*

**Response**: Thank you. We have fixed this.

**Minor comment #28:**

*– Fig 10: I don't understand what "% AEP" means. Isn't it just "%"?*

**Response**: AEP (Annual Exceedance Probability) is now defined in the text. As an example, a large flood which may be calculated to have a 1% chance to occur in any one year, is described as 1%AEP.[16]

**Minor comment #29:**

*– L 746: Shouldn't "P(Z2>z)" be "P(Z2>F_Z(u))"? Idem in Eq. (A.1)*

**Response**: Thank you. We have fixed this in the manuscript.[17]

[16] Line 454: As an example from Fig. 10, to design the highway with a failure probability of 1% annual exceedance probability (AEP), we would have to design each individual river crossing to a much rarer AEP of 0.25%

[17] Line 533: Assume that interest is in values above a threshold $u$ satisfying $P_u = 0.5$, in other words, $P\{Z_2 > u\} = P\{P_2 > P_u\} = 0.5$. In this case we have only one pair, at the index of 7, that satisfy both $P_1$ and $P_2$ are greater than $P_u = 0.5$, thus $P\{Z_1 > u, Z_2 > u\} = P\{P_1 > P_u, P_2 > P_u\} = 1/10 = 0.1$.

# Spatially dependent ~~Intensity-Duration-Frequency curves~~flood probabilities to support the design of civil infrastructure systems

**Phuong Dong Le[1,2], Michael Leonard[1], Seth Westra[1]**

[1]*School of Civil, Environmental and Mining Engineering, University of Adelaide, Adelaide, South Australia, Australia*

[2]*Thuyloi University, Hanoi, Vietnam*

*Email: lephuongdong_tb@tlu.edu.vn*

**Keywords: areal reduction factor, asymptotic independence, conditional probability, duration dependence, extreme rainfall, flood probability, inverted max-stable process, joint probability, spatially dependent Intensity-Duration-Frequency~~,~~**

**Abstract**

Conventional flood risk methods typically focus on estimation at a single location, which ~~is~~can be inadequate for civil infrastructure systems such as road or railway infrastructure. This is because rainfall extremes are spatially dependent, so that to understand overall system risk it is necessary to assess the interconnected elements of the system jointly. For example, when designing evacuation routes it is necessary to understand the risk of one part of the system failing given that another region is flooded or exceeds the level at which evacuation becomes necessary. Similarly, failure of any single part of a road section (e.g., a flooded river crossing) may lead to the wider system's failure (i.e. the entire road becomes inoperable). This study demonstrates a spatially dependent Intensity-Duration-Frequency ~~curve~~ framework that can be used to estimate flood risk across multiple catchments, accounting for dependence both in space and across different critical storm durations. The framework is demonstrated via a case study of a highway upgrade, comprising five ~~bridge~~river crossings~~ where the upstream contributing catchments each have different times of concentration.~~. The results show ~~that~~ substantial differences in conditional and unconditional design ~~flows can differ by a factor of two~~flow estimates, highlighting the importance of taking an integrated approach. There is also a reduction in the estimated failure probability of the overall system compared with the case ~~of no spatial dependence between storms.~~where each river crossing is treated independently. The results demonstrate the potential uses of

spatially dependent Intensity-Duration-Frequency ~~curves~~methods and suggest the need for more conservative design estimates to take into account conditional risks.

## 1. Introduction

Methods for quantifying the flood risk of civil infrastructure systems such as road and rail networks require considerably more information compared to traditional methods that focus on flood risk at a point. For example, the design of evacuation routes requires the quantification of the risk that one part of the system will fail at the same time that another region is flooded or exceeds the level at which evacuation becomes necessary. Similarly, a railway route may become impassable if any of a number of bridges are submerged, such that the 'failure probability' of that route becomes some aggregation of the failure probabilities of each individual section. Successful estimation of flood risk in these systems therefore requires recognition both of the networked nature of the civil infrastructure system across a spatial domain, as well as the spatial and temporal structure of flood-producing mechanisms (e.g. ~~storms and extreme rainfall) that can lead to system failure (e.g., Leonard et al. (2014), Seneviratne et al. (2012), Zscheischler et al. (2018)~~storms and extreme rainfall) that can lead to system failure (e.g., Leonard et al. (2014), Seneviratne et al. (2012), Zscheischler et al. (2018))).

One way to estimate such flood probabilities is to directly use information contained in historical streamflow data. For example, annual maximum streamflow at two locations might be assumed to follow a bivariate generalized extreme value distribution ~~(Favre et al., 2004; Wang, 2001; Wang et al., 2009)~~(Favre et al., 2004; Wang, 2001; Wang et al., 2009), which can then be used to estimate both conditional probabilities (e.g. the probability that one river is flooded given that the other river level exceeds a specified threshold) and joint probabilities (e.g. the probability that one or both rivers are flooded). Several frameworks have been demonstrated based directly on streamflow observations, including functional regression ~~(Requena et al., 2018)~~(Requena et al., 2018), multisite copulas ~~(Renard and Lang, 2007)~~(Renard and Lang, 2007), and spatial copulas ~~(Durocher et al., 2016)~~(Durocher et al., 2016). However,~~ this paper focuses on rainfall-based methods, as~~ in many instances continuous streamflow data are unavailable or insufficient at the locations of interest, or the catchment conditions have changed such that historical streamflow records as unrepresentative of likely future risk. For these situations, rainfall-based methods are often more appropriate.

~~To overcome common limitations~~There are two primary classes of ~~streamflow data,~~ rainfall-based ~~approaches are commonly used. One method~~methods to estimate flood probability. The first uses continuous rainfall data (either historical or generated) to compute continuous streamflow data using a rainfall-runoff model (Boughton and Droop, 2003; Cameron et al., 1999; ~~He et al., 2011; Hegnauer et al., 2014; Pathiraja et al., 2012)~~He et al., 2011; Hegnauer et al., 2014; Pathiraja et al., 2012), with flood risk then estimated based on the simulated streamflow time series. This method is computationally intensive and given the challenge of reproducing a wide variety of statistics across many scales, can have difficulties in modelling the dependence of extremes. Most spatial rainfall models operate at the daily timescale (Bárdossy and Pegram, 2009; Baxevani and Lennartsson, 2015; Bennett et al., 2016b; ~~Hegnauer et al., 2014; Kleiber et al., 2012; Rasmussen, 2013)~~Hegnauer et al., 2014; Kleiber et al., 2012; Rasmussen, 2013), whereas many catchments respond at ~~subdaily~~sub-daily timescales. ~~The~~This is likely to be because the capacity of space-time rainfall models to simulate the statistics of sub-daily rainfall remains a challenging research problem ~~(Leonard et al., 2008)~~(Leonard et al., 2008)~~. One,~~ although one approach is to exploit the relative abundance of data at the daily scale, then apply a downscaling model to reach ~~subdaily~~sub-daily scales ~~(Gupta and Tarboton, 2016)~~(Gupta and Tarboton, 2016). Continuous simulation is receiving ongoing attention and increasing application, yet there remain limitations when applying these models in many practical contexts.

~~A~~The second rainfall-based ~~approach~~method proceeds by applying probability calculations on rainfall, to construct ‘Intensity-Duration-Frequency’ (IDF) curves, which are then translated to a runoff event of equivalent probability ~~via~~ either via empirical models such as the rational method to estimate peak flow rate ~~(Kuichling, 1889; Mulvaney, 1851)~~(Kuichling, 1889; Mulvaney, 1851), or via event-based rainfall-runoff models that are able to simulate the full flood hydrograph (Boyd et al., 1996; Chow et al., 1988; ~~Laurenson and Mein, 1997)~~Laurenson and Mein, 1997). Regional frequency analysis is one type of method to estimate IDF ~~curves~~values, where the precision of at-site estimates is improved by pooling data from sites in the surrounding region ~~(Hosking and Wallis, 1997)~~(Hosking and Wallis, 1997). These methods can be combined with spatial interpolation methods to estimate parameters for any ungauged location of interest (Carreau et al., 2013). To determine an effective mean depth of rainfall over a catchment with the same exceedance probability as at a gauge location, the pointwise estimate of extreme rainfall is multiplied by an areal reduction factor (ARF) (Ball et al., 2016). However, such methods do not account for information on the spatial dependence of extreme rainfall—whether for a single storm duration, or for the more complex case of different durations across a region (Bernard, 1932; ~~Koutsoyiannis et al., 1998~~Koutsoyiannis et al., 1998). The ~~lack of dependence~~underlying independence assumption prevents these approaches from being applied to estimate conditional or joint flood risk at multiple points in a catchment or across several catchments, as would be required for a civil infrastructure system.

Although multivariate approaches can be tailored to estimate conditional and joint probabilities of extreme rainfall for specific situations (e.g., ~~Kao and Govindaraju (2008)~~Kao and Govindaraju (2008), ~~Wang et al. (2010)~~Wang et al. (2010), ~~Zhang and Singh (2007)~~Zhang and Singh (2007)), the development of a unified methodology that integrates with existing IDF-based flood estimation approaches remains elusive. This is particularly challenging given that it is not only necessary to ~~preserve~~account for dependence of rainfall across space, but also to account for dependence across storm burst durations, as different parts of the system may be vulnerable to different critical duration storm events. To this end, max-stable process theory has been demonstrated to represent storm-level dependence ~~(de Haan, 1984; Schlather, 2002)~~(de Haan, 1984; Schlather, 2002) and used to calculate conditional probabilities for a spatial domain ~~(Padoan et al., 2010)~~(Padoan et al., 2010). Copulas including the extremal-t copula ~~(Demarta and McNeil, 2005)~~(Demarta and McNeil, 2005), and the Husler-Reiss copula ~~(Hüsler and Reiss, 1989)~~(Hüsler and Reiss, 1989) have also been used to model rainfall dependence.

This study applies a max-stable approach with an emphasis on practical flood estimation problems~~:~~

~~1. The~~. To this end, any proposed approach needs to account for~~, not only the spatial dependence of rainfall ‘events’ of a single duration, but also the dependence across multiple durations. This was addressed by Le et al. (2018b), who linked the max-stable model of Brown and Resnick (1977) with the duration-dependent model of Koutsoyiannis et al. (1998), to create a model that could be used to reflect dependencies between nearby catchments of different sizes.~~:

**Formatted:** Normal, No bullets or numbering

1. ~~Given that often the interest is in rare flood events, the model needs to capture appropriate~~The spatial dependence of rainfall ‘events’ both for single durations, and also across multiple different durations. This was addressed by Le et al. (2018b), who linked a max-stable model with the duration-dependent model of Koutsoyiannis et al. (1998), to create a model that could be used to reflect dependencies between nearby catchments of different sizes.
2. The asymptotic properties of spatial dependence as the events become increasingly extreme, given the focus of many flood risk estimation methods on rare flood events. Recent evidence is emerging that rainfall has an asymptotically independent characteristic ~~(Le et al., 2018a; Thibaud et al., 2013)~~(Le et al., 2018a; Thibaud et al., 2013), which means that the level of the rainfall’s dependence reduces with an increasing return period ~~(Wadsworth and Tawn, 2012)~~(Wadsworth and Tawn, 2012). The requirement of asymptotic independence indicates that inverted max-stable models are preferable over max-stable models.

This study adapts the methods developed by ~~Le et al. (2018b)~~Le et al. (2018b) to inverted max-stable models to derive spatially-dependent IDF ~~curves~~estimates and ARFs as the basis for transforming rainfall into flood flows. The approach is demonstrated on a highway system spanning 20 km with five separate ~~bridge crossings, and with the contributing catchment at each crossing having a different time of concentration.~~river crossings.

The case study is designed to address two related questions: (i) “What flood flow needs to be used to design a bridge that will fail on average only once on average every $M$ times ~~(e.g., $M = 10$ for a 10-year event)~~ given that a neighbouring catchment is flooded?”; and (ii) “What is the probability that the overall system fails given that each bridge is designed to a specific exceedance probability event (e.g., the 1% annual exceedance probability event)?” The method for resolving these questions represents a new ~~paradigm in which~~approach to estimate flood risk for engineering design, by focusing attention on the risk of the entire system, rather than the risk of individual system elements in isolation.

In the remainder of the paper, Section 2 emphasises the need for spatially dependent IDF ~~curves~~estimates in flood risk design, followed by Section 3 which outlines the case study and data used. Section 4 explains the ~~methodology~~implementation of the framework, including a method for analysing the spatial dependence of extreme rainfall across different durations. ~~It also includes an algorithm with which to use that information in estimating the conditional and joint probabilities of floods. The results, and a discussion on the behaviour of flood~~Results on the behaviour of floods due to the spatial and duration dependence of rainfall extremes, are provided in Section 5. Conclusions and ~~recommendations~~discussion follow in Section 6.

## 2. The need for spatially dependent IDF ~~curves~~estimates in flood risk estimation

The main limitation of conventional methods of flood risk estimation is that they isolate bursts of rainfall and break the dependence structure of extreme rainfall. Figure 1 demonstrates a traditional process of estimating at-site extreme rainfall for two locations (gauge 1, gauge 2) and three durations (1, 3, and 5 hr) ~~(Stedinger et al., 1993)~~(Stedinger et al., 1993). The process first involves extracting the extreme burst of rainfall for each site, duration and year from the continuous rainfall data, and then fitting a probability distribution (such as the Generalised Extreme Value (GEV) distribution) to the extracted data. Figure 1 demonstrates that, through the process of converting the continuous rainfall data to a series of discrete rainfall 'bursts', this process breaks ~~both~~ the dependence both with respect to duration and space. Firstly, the duration dependence is broken by extracting each duration separately, whereas for the hypothetical storm in Fig. 1 it is clear that the annual maxima from some of the extreme bursts come from the same storm. Secondly, the spatial dependence is broken because each site is analysed independently. Again, for the hypothetical storm of Fig. 1 it can be seen that the 5 hr storm has occurred at the same time across the two catchments, and this information is lost in the subsequent probability distribution curves. Lastly, there is cross-dependence in space and duration. For example, the 1 hr extreme from gauge 2 occurs at the same time as the 5 hr extreme from gauge 1. This may be relevant if there are two catchments with times of concentration matching 1 hr and 5 hr respectively, which can arise where catchments are neighbouring or nested.

Formatted: English (United States)

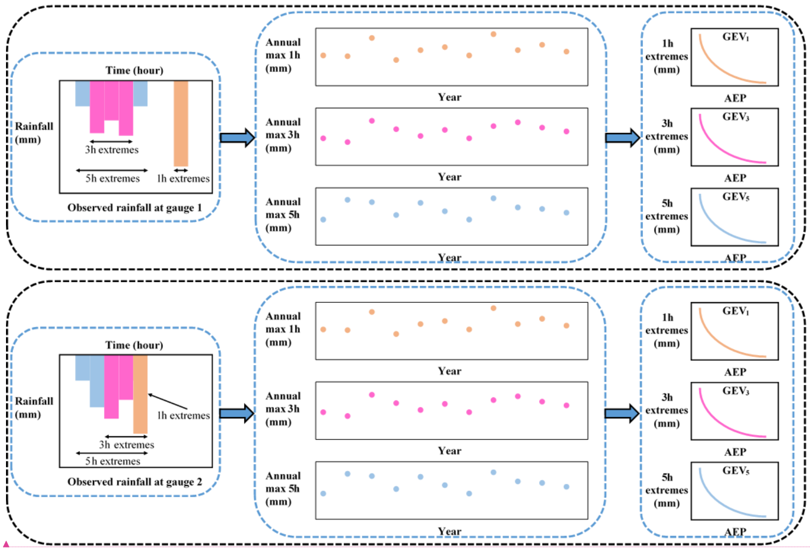


**Figure 1.** Illustration of process to estimate rainfall extremes for each individual location in conventional flood risk approach, the upper panel is for gauge 1 and the lower panel is for gauge 2.

Having obtained the IDF ~~curves~~estimates for individual locations in Fig. 1, the next step is commonly to convert this to spatial IDF maps by interpolating results between gauged locations. Figure 2 shows hypothetical IDF ~~curves~~maps from individual sites, with a separate spatial contour map usually provided for each storm burst duration. In a conventional application the respective maps are used to estimate the magnitude of extreme rainfall over catchments for a specified time of concentration. The IDF ~~curves~~estimates are combined with an areal reduction factor (ARF) to determine the volume of rainfall over a region (since rainfall is not simultaneously extreme at all locations over the region). However, because the spatial dependence was broken in the IDF analysis ~~of IDF curves~~, the ~~ARF~~ARFs come from a separate analysis and are an attempt to correct for the broken spatial relationship within a catchment (Bennett et al., 2016a). Lastly, the rainfall volume over the catchment is combined with a temporal pattern (i.e. the distribution of the rainfall hyetograph within a single 'storm burst') and input to a runoff model to simulate flood-flow at a catchment's outlet. Where catchment flows can be considered independently this process has been acceptable for conventional design, but because this process does not account for dependence across durations and across a region, it is not possible to address problems that span multiple catchments, as with civil infrastructure systems.

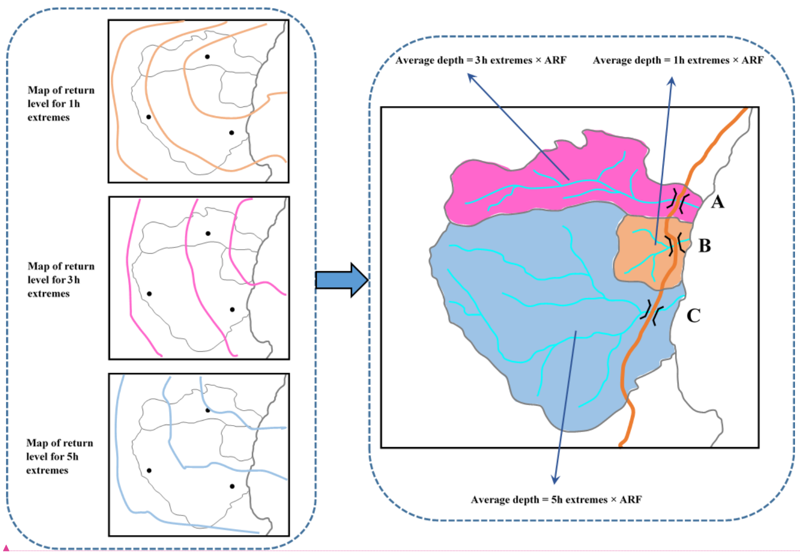


**Figure 2.** Illustration of map of return level and how to use it in estimating flood flow in conventional flood risk estimates approach.

The process in Fig. 1 breaks out the dependence of the observed rainfall, which makes the conventional approach unable to analyse the dependence of flooding at two or more separate locations. Instead, this paper advocates for spatially dependent IDF ~~curves which~~estimates that are developed by retaining the dependence of observed rainfall in the estimation of extremal rainfall. By applying spatially dependent IDF ~~curves~~estimates to a rainfall-runoff model, it becomes possible to represent the dependence of flooding between separate locations~~ can be achieved~~.

## 3. Case study and data

The region chosen for the case study is in the mid north coast region of New South Wales, Australia. This region has been the focus of a highway upgrade project and has an annual average daily traffic volume on the order of 15,000 vehicles along the existing highway. The upgrade traverses a series of

**Formatted:** English (United States)

coastal foothills and floodplains for a total length of approximately 20 km. The project's major river crossings consist of extensive floodplains with some marsh areas.

The case study has five main catchments that are numbered in sequence in Fig. 3: (1) Bellinger, (2) Kalang River, (3) Deep Creek, (4) Nambucca and (5) Warrell Creek. The area and time of concentration of these catchments is summarised in Table 1, with the latter estimated using the ratio of the flow path length and average flow velocity ~~(SKM, 2011)~~(SKM, 2011). The Deep Creek catchment has a time of concentration of 8~~.3~~ hr, while the other four catchments have much longer times of concentration, ranging from 27~~.8~~ to 38~~.9~~ hr. ~~These require the estimates of~~ The differing durations indicate that it is necessary to consider spatial dependence across ~~different~~ this range of durations ~~of rainfall extremes. Although the~~to estimate joint and conditional flood risk. The spatial dependence across rainfall durations ~~would be~~is expected to be lower than across a single duration, since short- and long-rain events are often driven by different meteorological mechanisms ~~(Zheng et al., 2015)~~(Zheng et al., 2015)~~, it is nonetheless likely that~~. However some ~~level of~~ spatial dependence ~~would exist and need~~ is still likely to be ~~integrated into the risk calculations. This is particularly of relevance~~present, given that extremal rainfall in ~~this~~the region is strongly associated with 'east coast low' systems off the eastern coastline, whereby extreme hourly rainfall bursts are often embedded in heavy multi-day rainfall events.

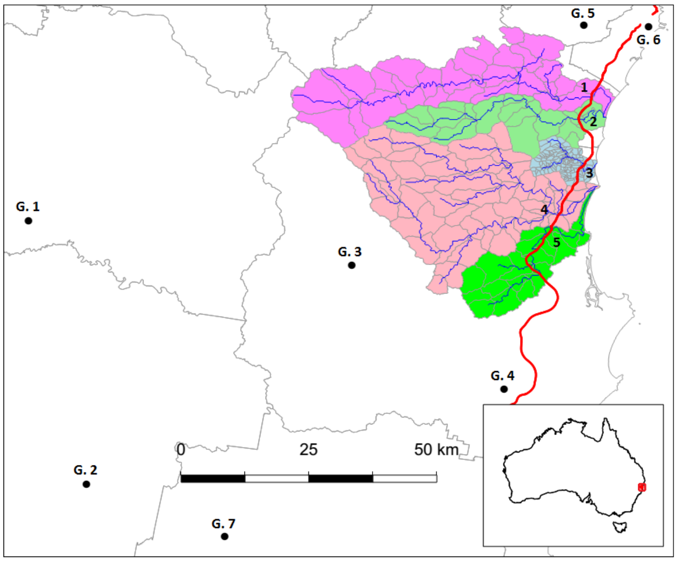


**Figure 3.** Map of the case study in New South Wales, Australia. The black dots indicate the rainfall gauges (G. 1 to G. 7), the red line indicates the Pacific Highway upgrade project, and the blue lines indicate the main river network. The numbers from one to five indicate the locations of the main river crossings.

**Formatted:** English (United States)

**Table 1.** Summary of ~~properties for~~case study catchments ~~in the case study~~properties .

| No. | Catchment | Area (~~ha~~km$^2$) | ~~Raw time~~Time of concentration (hour) |
|---|---|---|---|
| 1 | Bellinger | ~~77150~~772 | 37 |
| 2 | Kalang River | ~~34140~~341 | 33 |
| 3 | Deep Creek | ~~9180~~92 | 8 |
| 4 | Nambucca (upper) | 1020~~102015~~ | 38 |
| 5 | Warrell Creek | ~~29440~~294 | 27 |

**Formatted Table**

The black circles in Fig. 3 represent the sub-daily rain stations used for this study. There were ~~7~~seven sub-daily stations selected, with 35 years of record in common for the whole region. The data was available at a 5 minute interval and aggregated to longer durations. For convenience in comparing the times of concentration between the catchments, this study assumes a time of concentration of 9 hr for the Deep Creek catchment, while identical times of concentration of 36 hr are assumed for the other four catchments.

## 4. Methodology

This section ~~provides~~describes the method used to estimate the conditional and joint probabilities of ~~flood~~streamflow for civil infrastructure systems based on rainfall extremes, ~~which is explained according to~~ with the sequence of steps ~~shown~~illustrated in Fig. ~~4. First, the~~4. The overall aim is to estimate rainfall exceedance probabilities and corresponding flow estimates that account for dependence across multiple catchments. The generalized Pareto distribution (GPD) is used as the marginal distribution to fit to observed rainfall for all ~~duration~~durations at each ~~locations~~location (Section 4.1). ~~After that~~An extremal dependence model is required to evaluate conditional and joint probabilities. Here, an inverted max-stable process is ~~introduced and then~~used with dependence not only in space but also in duration (Section 4.2). The fitted ~~to rainfall extremes of identical or different durations (Sections 4.2 & 4.3). The conditional and joint probabilities~~model is evaluated in a range of ~~rainfall are then estimated in Section 4.4, which is followed by~~contexts, including the ~~simulation to calculate~~ construction of joint and conditional return level maps. The derivation of areal reduction ~~factor (ARF) in~~ factors and joint rainfall estimates are made with the assistance of simulations based on the fitted model (Section 4.~~5.~~3). An event-based rainfall-runoff model is employed in Section 4.~~6~~4 to transform ~~conditional rainfall to conditional~~extremal design rainfalls to corresponding flows.~~ With an assumption that there is a one-to-one correspondence between rainfall intensity and flow rate, the joint flood probability for the case study is equal to the joint probability of rainfall. An analysis for the independent model (the case of complete independence) is also implemented for comparison.~~

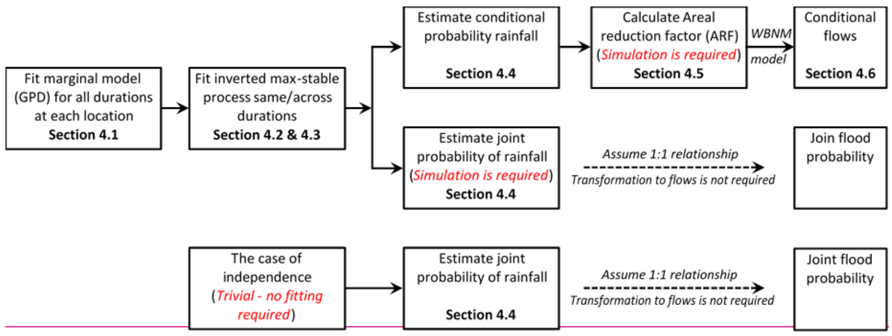

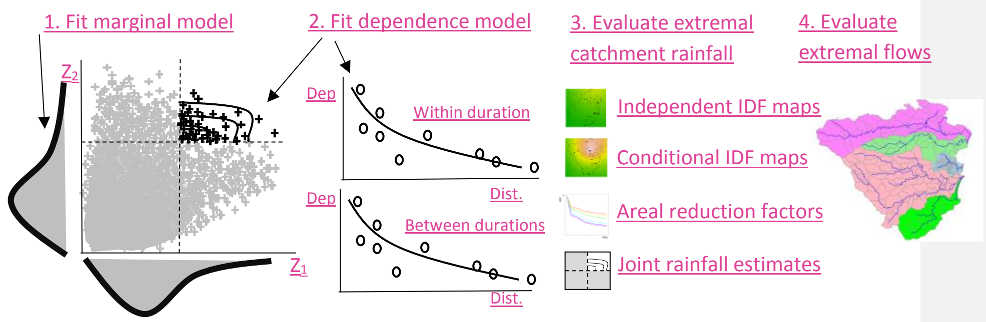


**Figure 4.** The flow chart for the overall methodology.

### *4.1. Marginal model for rainfall*

This study defines extremes as those greater than some threshold $u$. For large $u$, the distribution of $Y$ conditional on $Y > u$ may be approximated by the generalized Pareto distribution (GPD) ~~(Pickands, 1975~~(Pickands, 1975; Davison and Smith, 1990; ~~Thibaud et al., 2013)~~Thibaud et al., 2013):

$$G(y) = 1 - \left\{1 + \frac{\xi(y-u)}{\sigma_u}\right\}^{-1/\xi}, \quad y > u, \tag{1}$$

defined on $\{y: 1 + \xi(y-u)/\sigma_u > 0\}$ where $\sigma_u > 0$ and $-\infty < \xi < +\infty$ are scale and shape parameters, respectively. The probability that a level $y$ is exceeded is ~~then~~ $\Phi_u\{1 - G(y)\}$, where $\Phi_u = \Pr(Y > u)$.

The selection of the appropriate threshold $u$ involves a trade-off between bias and variance. A threshold that is too low leads to bias because the GPD approximation is poor. A threshold too high leads to high variance because of a small number of excesses. Two diagnostic tests are used to determine the appropriate threshold $u$: the mean residual life plot and the parameter estimate plot (Coles, 2001; Davison and Smith, 1990). These methods use the stability property of a GPD, so that if a GPD is valid for all excesses above $u$, then excesses of a threshold greater than $u$ should also follow a GPD~~. Detailed guidance of these methods can be found in~~ (Coles ~~(~~, 2001)~~.~~. To construct IDF maps across the region, the parameters of the GPD are interpolated across the region using a thin plate spline with covariates of longitude and latitude. Though more detailed modelling of covariates could be used to improve estimates (Le et al. 2018b), the interpolation used here is sufficient for demonstrating the overall method.

### *4.2. Dependence model for spatial rainfall*

Consider rainfall as a stationary stochastic process $Z_i$ associated with a location $x_i$ ~~in~~and a ~~region of interest~~specific duration (the notation ~~for the stochastic process~~ is simplified from $Z(x_i)$ to $Z_i$).~~ Without loss of generality it can be assumed that the margins of $Z$ have a unit Fréchet distribution.~~ An important property of dependence in the extremes is whether or not two variables are likely/unlikely to co-occur as the extremes become rarer, as this can significantly influence the estimate of frequency for flood events of large magnitude. This is referred to as asymptotic dependence/independence, respectively. For the case of asymptotic independence, the dependence structure becomes weaker as the extremal threshold increases, which is ~~formally~~ defined as $\lim_{z\to\infty} P\{Z_1 > z | Z_2 > z\} = 0$ for all $x_1 \neq x_2$. The spatial extent of a rainfall event with asymptotically independent extremes will diminish as its rarity increases.

~~An example of~~ This study uses an asymptotically independent model~~ is~~, of which there are multiple types including the Gaussian copula (Davison et al., 2012) and inverted max-stable ~~process~~processes ~~(Wadsworth and Tawn, 2012)~~(Wadsworth and Tawn, 2012). ~~A general description of all continuous~~ This study uses an inverted Brown-Resnick max-stable ~~processes that have standard exponential margins on a spatial domain $X$ is~~

$$\cancel{\tilde{\Omega}(x) = \min_{k\geq 1} U_k/W_k, \quad x \in X, \qquad (2)}$$

~~where $U_k$ are points of a unit Poisson~~ process~~ on $(0,\infty)$ and the $W_k(x)$ are independent replicas of a continuous, non-negative stochastic process $W(x)$ in the spatial domain $X$, with $E\{W(x)\} = 1$ for all $x \in X$.~~

~~It is convenient to work with a simple inverted max-stable process with unit Fréchet margins, because the marginal distribution can easily be transformed back to the GPD scale. To transform the process $\tilde{\Omega}(x)$ to unit Fréchet margins, the following transformation is used:~~

$$\cancel{\Omega(x) = -\frac{1}{\log\{1 - e^{-\tilde{\Omega}(x)}\}}, \quad x \in X,} \qquad \cancel{(3)}$$

~~then $\Omega(x)$ is an asymptotically independent process with unit Fréchet margins.~~

~~From Eq. (2), different models for $W$ give different inverted max-stable processes. There are two popular and easily simulated classes of model for the inverted max-stable processes: the Brown-Resnick model~~ (Asadi et al., 2015~~; Huser and Davison, 2013; Kabluchko et al., 2009; Oesting et al., 2017)~~; Huser and Davison, 2013; Kabluchko et al., 2009; Oesting et al., 2017)~~, and extremal-t model (Opitz, 2013). This study uses the Brown-Resnick form of equations from the family of an inverted max-stable process because Le et al. (2018a) showed it has better performance than the extremal-t model.~~ based on a performance evaluation summarised in Le et al. (2018a).

Formatted: Font: +Body (Calibri)

~~***4.3. Fitting the dependence model***~~

~~One simple way to calibrate dependence models is to fit them to data by matching a suitable statistic.~~ The dependence structure of the inverted max-stable process is represented by the pairwise residual tail dependence coefficient ~~(Ledford and Tawn, 1996)~~(Ledford and Tawn, 1996).

For a generic continuous process $Z_i$ for a given duration and associated with a specific location $x_i$, the empirical pairwise residual tail dependence coefficient $\eta$ for each pair of locations $(x_1, x_2)$ is

$$\eta(x_1, x_2) = \cancel{\lim_{y\to\infty} \frac{\log P\{Z_2 > z\}}{\log P\{Z_1 > z, Z_2 > z\}}} \lim_{z\to\infty} \frac{\log P\{Z_2 > z\}}{\log P\{Z_1 > z, Z_2 > z\}}. \qquad (42)$$

The value of $\eta \in (0,1]$ indicates the level of extremal dependence between $Z_1$ and $Z_2$ (Coles et al., 1999), with lower values indicating lower dependence. An example of how to calculate the residual tail dependence coefficient is provided in Appendix A for a sample dataset.

To estimate the dependence structure of an inverted max-stable model, the theoretical residual tail dependence coefficient function is ~~usually~~ fitted to its empirical counterpart. Here the residual tail dependence coefficient function is assumed to only depend on the Euclidean distance between two locations $h = \|x_1 - x_2\|$. The theoretical residual tail dependence coefficient function for the inverted Brown-Resnick model is given as:

$$\eta(h) = \frac{1}{2\Phi\left\{\sqrt{\frac{\gamma(h)}{2}}\right\}},$$ (~~5~~3)

where $\Phi$ is the standard normal cumulative distribution function, $h$ is the distance between two locations, and $\gamma(h)$ belongs to the class of variograms $\gamma(h) = \|h\|^{\beta}/q$ for $q > 0$ and $\beta \in (0,2)$. The ~~models are then~~model is fitted to the empirical residual tail dependence ~~coefficients~~coefficient by modifying parameters $q$ and $\beta$ until the sum of squared errors is minimized.

~~In the case that extreme rainfall at locations $x_1$ and $x_2$ are of identical duration (i.e. both 36 hr), then the~~The inverted max-stable process is fitted to the observations by minimizing the sum of the squared errors of the residual tail dependence coefficients. ~~This information can be directly applied to the case where two catchments have a similar time of concentration owing to their similar shape and size. However, there are many instances when two catchments of interest will have differing times of concentration; in particular, when~~When the extreme rainfall at location $x_1$ and $x_2$ are of different durations ~~(e.g., 36 hr and 9 hr),~~, the dependence is less than ~~the case of 36 hr and 36 hr. This observation is evident when considering the special case of a single location, i.e.~~ when the extremes are of the same ~~point is considered twice~~duration. For example, at a ~~distance of $h = 0$. For the case where~~single location ($h$ = 0), when the duration is the same, the rainfall values are identical and have perfect dependence, but when the duration of extremes are different the values are not identical and the dependence is less. ~~Therefore, an~~An adjustment needs to be made to ~~ensure that~~ the theoretical pairwise residual tail dependence coefficient function ~~suitably represents the observed pairwise residual tail dependence coefficients for the case of~~when extreme rainfalls ~~of~~have different durations.

Following ~~Le et al. (2018b)~~Le et al. (2018b), an adjusted approach is used by adding a nugget to the ~~variograms~~variogram as:

$$\gamma_{ad.}(h) = h^{\beta}/q + c(D - d)/d,$$ (~~6~~4)

where $h$, $\beta$, and $q$ are the same as those in Eq. (~~5~~3); $d$ is the duration (in hours); $0 < d \leq D$, where $D$ is the maximum duration of interest (e.g. $D = 36$ hr for the case study described in this paper); and $c$ is a ~~parameters~~parameter to adjust dependence according to duration. This adjustment is intended to condition the behaviour of shorter duration extremes on a $D$-hour extreme of ~~a~~ specified magnitude. It is constructed to reflect the fact that when compared to a $D$-hour extreme, a shorter duration results in less extremal dependence. Cases involving conditioning of longer periods on shorter periods (such as a 36 hr extreme given a 9 hr extreme has occurred) can also use the relationship in Eq. (~~6~~4), but with different parameter values.

To fit the inverted max-stable process for all pairs of durations at locations $x_1$ and $x_2$ (i.e. 36 hr and 12 hr, 36 hr and 9 hr, 36 hr and 6 hr, 36 hr and 2 hr, 36 hr and 1 hr), the theoretical pairwise residual tail dependence coefficient function in Eq. (~~5~~3) is used with the adjusted variogram from Eq. (~~6~~4) where the parameters $\beta$ and $q$ are first obtained from the fitted results of the case of identical 36 hr durations at location $x_1$ and $x_2$. The parameter $c$ is obtained by a least square fit of the residual tail dependence coefficient across all durations.

### ***4.~~4. Estimate~~3. Simulation based estimation of ~~conditional~~areal and joint ~~probabilities of~~ rainfall ~~extremes~~***

The dependence model specification in the previous section enables the calculation of joint and conditional ~~probability $P\{Z_2 > z_2 | Z_1 > z_1\}$ is obtained from the bivariate inverted max-stable process cumulative distribution function (CDF) in unit Fréchet margins~~ (Thibaud et al., 2013)~~, which is given as:~~

$$P\{Z_1 \le z_1, Z_2 \le z_2\} = 1 - \exp\left\{-\frac{1}{g_1}\right\} - \exp\left\{-\frac{1}{g_2}\right\} + \exp[-V\{g_1, g_2\}], \qquad (\cancel{7})$$

~~where $g_1 = -1/\log\{1-\exp(-1/z_1)\}$, $g_2 = -1/\log\{1-\exp(-1/z_2)\}$, and the exponent measure $V$~~ (Padoan et al., 2010) ~~is defined as:~~

$$V\{g_1, g_2\} = -\frac{1}{g_1}\Phi\left\{\frac{a}{2} + \frac{1}{a}log\frac{g_2}{g_1}\right\} - \frac{1}{g_2}\Phi\left\{\frac{a}{2} + \frac{1}{a}log\frac{g_1}{g_2}\right\}. \qquad \cancel{(8)}$$

~~In Eq. (8), $\Phi$ is the standard normal cumulative distribution function, $a = \sqrt{2\gamma_{aa}(h)}$ with $\gamma_{aa}(h)$ is the variograms that was mentioned in the explanation of Eq. (6).~~

~~In unit Fréchet margins, the relationship between the~~probabilities (Appendix B). Therefore, in addition to traditional IDF return level ~~$z$~~maps that are based on independence between locations and ~~the return period $T$ is given as $z = -1/log(1-1/T)$, and the conditional probability for the max-stable process can then be estimated~~durations, it is possible to account for the coincidence of rainfall within the region. Current design procedures using~~:~~

~~$P\{Z_2 > z_2 | Z_1 > z_1\} = T_1 \left[\frac{1}{T_1} - \exp\left(-\frac{1}{z_2}\right) + P\{Z_1 \le z_1, Z_2 \le z_2\}\right],$~~ ~~(9~~ IDF estimates are event-based and rely on ancillary steps to reconstruct elements of the design storm that were )

~~where $T_1$ is the return period corresponding to the return level $z_1$.~~

~~The joint probability for independent variables is~~ broken ~~down as the product of the marginals. The probability that there is at least one location that has an extreme event exceeding a given threshold for the case that all of events are independent can be calculated based on the addition rule for the union of probabilities, as:~~

$$P(Z_1 > z_1 \text{ or} \dots \text{or } Z_N > z_N) = \sum_{i=1}^{N} P(Z_i > z_i) - \sum_{i<j} P\big(Z_i > z_i, Z_j > z_j\big) + \cdots$$

$$+(-1)^{N-1} P(Z_1 > z_1, \dots, Z_N > z_N), \qquad \text{~~(10)~~}$$

~~where $N$ is the number of locations, and $P(Z_1 > z_1, \dots, Z_N > z_N) = P(Z_1 > z_1) \dots P(Z_N > z_N)$, because all of the events are independent.~~

### ***~~4.5. Areal reduction factor~~ during the estimation ~~and simulation~~ procedure ~~for spatial rainfall~~***

~~Before transforming extreme rainfall to flood flow through an event-based model,~~. One critical element is the areal reduction ~~factors (~~factor (ARF), which the dependence model can also be used to estimate. ARFs~~) were employed~~ are used to ~~make the adjustment of~~adjust rainfall ~~depth~~ at a point (~~i.e.~~such as the centroid of a catchment) ~~for a given return level estimate, to~~ to an effective ~~(~~mean~~) depth~~ rainfall over ~~a~~the catchment with ~~the same~~equivalent probability of exceedance ~~as the single point~~ (Ball et al., 2016~~; Le et al., 2018a)~~; Le et al., 2018a). ARFs can be estimated from observed rainfall data, but it is difficult to extrapolate ~~ARFs~~them for long return periods from observations with just 35 years of record for this study. To deal with this difficulty and to analyse the asymptotic behaviour of ARFs, ~~Le et al. (2018a)~~Le et al. (2018a) proposed a framework to simulate ARFs ~~for long return periods by~~ using ~~an~~the same inverted~~-~~max~~-~~stable process~~, which is applied~~ model adopted here ~~for durations of 36 and 9 hrs.~~

. The simulation procedure ~~for spatial rainfall for a given duration is implemented in~~ from Le et al. (2018a) is summarised according to two steps. In the first step, the theoretical residual tail dependence coefficient function in Eq. (~~5~~3) is fitted to observed rainfall for the duration of interest to obtain the variogram parameters $q > 0$ and $\beta \in (0,2)$. The inverted Brown-Resnick process ~~with unit Fréchet margins is then simulated~~ is obtained from a simulation of the Brown-Resnick process using the algorithm of ~~Dombry et al. (2016)~~Dombry et al. (2016) over a spatial domain ~~and the inverted Brown-Resnick process with unit Fréchet margins is obtained through Eq. (2) and Eq. (3)~~. In the second step, the simulation in step 1 is transformed from unit Fréchet margins to the rainfall scaled margins~~.~~ (inverse transformation of Eq. (B.1) in Appendix B). For rainfall magnitudes above the threshold the generalised Pareto distribution in Eq. (1) is used, and below the threshold the empirical distribution is used. The empirical distributions at ungauged sites are derived from the nearest gauged sites and using ~~a~~the interpolated response surface ~~(latitude and longitude covariates) to spatially interpolate~~of the GPD threshold parameter.

An advantage of ~~this~~the simulation approach is that it can reflect the proportion of dry days in the empirical distribution by making the simulated rainfall contain zero values ~~(Thibaud et al., 2013)~~(Thibaud et al., 2013). Another advantage is that ~~this approach~~ the use of empirical distributions guarantees that the marginal distributions of simulated rainfall below the threshold ~~matches~~match the observed marginal distributions. There may be a drawback ~~of this approach~~ by forcing the simulated rainfall to have the same extremal dependence structure for both parts below and above the threshold, which may not be true for non-extreme rainfall. However, the dependence structure of non-extreme rainfall contributes insignificantly to extreme events ~~(Thibaud et al., 2013)~~(Thibaud et al., 2013) and is unlikely to affect the results.

For calculating ARFs, the simulation is implemented separately for spatial rainfall of 36 and 9 hrs duration. ~~After the simulated spatial rainfall for 36 and 9 hrs are respectively obtained,~~ ARFs are calculated for each duration and different return periods, which can be found in the supplementary material (Fig. S1 and S2). Figure S1 and S2 provide relationships between ARFs and area (in km$^2$) for different return periods for the case study catchments~~. These relationships are calculated through the simulation of~~ simulated using the inverted Brown-Resnick process over equally sized grid points. The relationships are interpolated to obtain the ARFs for each ~~of subcatchments (corresponding to respective areas 91 km$^2$, 294 km$^2$, 341 km$^2$, 771 km$^2$,~~ subcatchment. ~~1020 km$^2$). When the interest is in the joint probability of rainfall extremes of different durations, the simulation of spatial rainfall should be implemented across multiple durations. In this case, each term of the covariance matrix is calculated from the dependence structure of the corresponding pair of locations. In detail, the covariance matrix of the simulation procedure provided by Dombry et al. (2016) is calculated from the variogram in Eq. (6). The covariance element for a pair of locations with the same duration (e.g. 36 and 36 hr) is calculated from the variogram of identical durations for 36 and 36 hr. The covariance element for a pair of locations with different durations (e.g. 36 and 9 hr) is calculated from the variogram across durations for 36 and 9 hr.~~

The recommended approach for estimating the overall failure probability of a system is demonstrated by considering a hypothetical traffic system with multiple river crossings at locations. If there is a one-to-one correspondence between extreme rainfall intensity over a catchment and flood magnitude, the overall failure probability will be approximately equal to the probability that there is at least one river crossing whose contributing catchment has rainfall extremes exceeding the design level, which can be estimated using simulations of the spatial rainfall model. Given the different times of concentration in each catchment, the simulation must account for extremes of different durations. Specifically, the covariance matrix of the simulation procedure provided by Dombry et al. (2016) is calculated from the variogram in Eq. (3). The covariance element for a pair of locations with the same duration (e.g. 36 and 36 hr) is calculated from the variogram of identical durations for 36 and 36 hr. The covariance element for a pair of locations with different durations, for example 36 and 9 hr, is calculated from the variogram across durations for 36 and 9 hr. A set of 10,000 years simulated rainfall is generated from the fitted model to calculate the overall failure probability of a highway section (Eq. B.5). The process is repeated

100 times to estimate the average failure probability, under the assumption that all river crossings of the highway are designed to the same individual failure probability.

### *4.~~6~~4. Transforming rainfall extremes to flood flow*

To estimate flood flow from rainfall extremes, the Watershed Bounded Network Model (WBNM) (Boyd et al., 1996), is employed~~ in this study.~~. WBNM calculates flood runoff from rainfall hyetographs that represent the relationship between the rainfall intensity and time (Chow et al., 1988). It divides the catchment into subcatchments, allowing hydrographs to be calculated at various points within the catchment, and allowing the spatial variability of rainfall and rainfall losses to be modelled. It separates overland flow routing from channel routing, allowing changes to either or both of these processes, for example in urbanised catchments. The rainfall extremes are estimated at the centroid of the catchment, and are converted to average spatial rainfall using the simulated ARFs described in Section 4.~~5 before estimation of the rainfall hyetographs.~~3. Design rainfall hyetographs are used to convert the rainfall magnitude to absolute values through the duration of a storm following standard design guidance in Australia (Ball et al., 2016).

Hydrological models (WBNM) for the case study area were developed and calibrated in previous studies ~~(WMAWater, 2011)~~(WMAWater, 2011). Hydrological model layouts for the Bellinger, Kalang River, Nambucca, Warrell and Deep Creek catchments can be found in the supplementary material (Fig. S3 to S5).

## 5. Results ~~and discussion~~

### *5.1. Evaluation of model for space-duration rainfall process*

A GPD with an appropriate threshold was fitted to the observed rainfall data for 36 hr and 9 hr durations, and the Brown-Resnick inverted max-stable process model was calibrated to determine the spatial dependence.

Analysis of the rainfall records led to the selection of a threshold of 0.98 for all records as reasonable across the spatial domain and the GPD was fitted to data above the selected threshold. Figure 5 shows QQ plots of the marginal estimates for a representative station for two durations (36 and 9 hr~~.~~). Overall the quality of fitted distributions is good and plots for all other stations can be found in the supplementary material (Fig. S6 and S7).

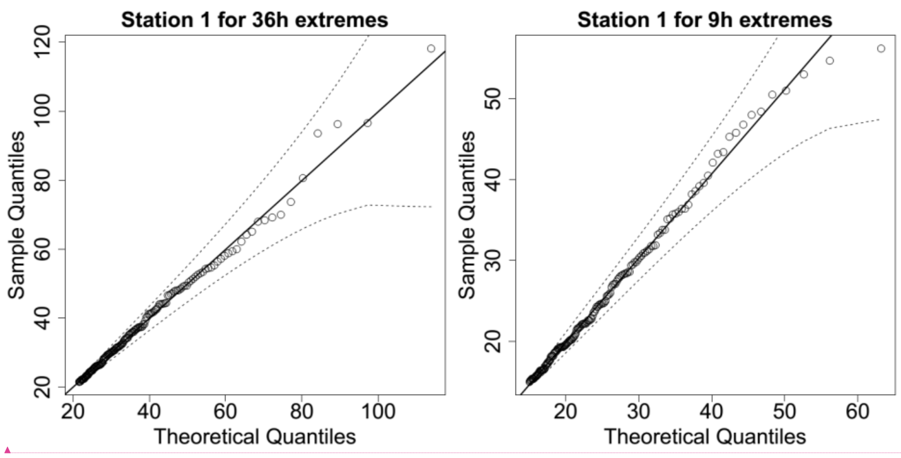


Formatted: English (United States)

**Figure 5.** QQ plots for the fitted GPD at one representative station, dotted lines are the 95% confidence bounds, and the solid diagonal line indicates a perfect fit.

The inverted max-stable process across different durations was calibrated to determine dependence parameters. The theoretical pairwise residual tail dependence coefficient function between two locations ($x_1$ and $x_2$) was calculated based on Eq. (~~5~~3) and Eq. (~~6~~4), and the observed pairwise residual tail dependence coefficient $\eta$ was calculated using Eq. (~~4~~2). Figure 6 shows the pairwise residual tail dependence coefficients for the Brown-Resnick inverted max-stable process versus distance. The black points are the observed pairwise residual tail dependence coefficients, while the red lines are the fitted pairwise residual tail dependence coefficient functions. A coefficient equal to 1 indicates complete spatial dependence, and a value of 0.5 indicates complete spatial independence. The top-left panel shows the dependence between 36 hr extremes across space, with the distance $h$ = 0 corresponding to "complete dependence". It also shows the dependence decreasing with increasing distance. Figure 6 indicates that the model has a reasonable fit to the observed data given the small number of dependence parameters. Although the theoretical coefficient (red line) does not perfectly match at long distances, the main interest for this case study is in short distances, ~~especially~~including at $h = 0$ for the case of dependence between two different durations at the same location.

The remaining panels of Fig. 6 show the dependence of 36 vs. 9 hr extremes, 36 vs. 6 hr extremes, and 36 vs. 3 hr extremes, with the latter two duration combinations not being used directly in the study but nonetheless showing the model performance across several durations. As expected, the dependence levels are weaker compared with 36 vs. 36 hr extremes at the same distance, especially at zero distance. ~~This is expected, as the dependence at the same site between exceedances at different durations will be lower than between exceedances at the same duration. This is because exceedances of different durations may arise from different storm events (Zheng et al., 2015).~~This is expected, as extremes of different durations are more likely to arise from different storm events compared to storms of the same duration.

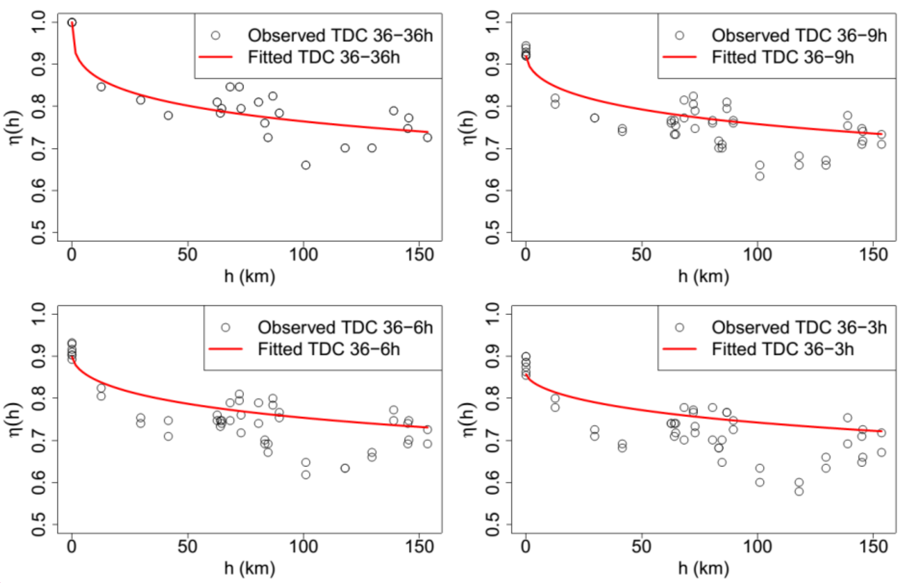


**Figure 6.** Plots of pairwise residual tail dependence coefficient (TDC) against distance for 36 hr extremes and 36 hr extremes (top left), for 36 hr extremes and 9 hr extremes (top right), for 36 hr extremes and 6 hr extremes (bottom left), and for 36 hr extremes and 3 hr extremes (bottom right). The black points are estimated residual tail dependence coefficients for pairs of sub-daily stations, and the red lines are theoretical residual tail dependence coefficient function.

### *5.2. Estimating conditional rainfall ~~extremes~~return levels and corresponding conditional flows for evacuation route design*

**Formatted:** English (United States)

**Formatted:** Justified

The recommended approach for estimating conditional rainfall extremes is demonstrated by considering a hypothetical evacuation route across location $x_2$, given a flood occurs at location $x_1$, evaluated using Eq. (~~9~~B.4). This approach is applied to a case study of the Pacific Highway upgrade project that contains five main river crossings (from Fig. 3). For evacuation purposes, we need to know "what is the probability that a bridge fails only once on average every $M$ times (e.g., $M = 10$ for ~~an~~a one in 10 chance conditional event) ~~that its~~when a neighbouring bridge is flooded?" This section provides the conditional estimates for two pairs of neighbouring bridges in the case study that have the shortest Euclidean distances, i.e. pairs $(x_1, x_2)$ and $(x_2, x_3)$. The comparisons of unconditional and conditional maps are given in Fig. 7 and Fig. 8, and the corresponding unconditional and conditional flows are given in Fig. 9. ~~In order to obtain the maps in Fig. 7 and Fig. 8, a thin plate spline regression against longitude and latitude was employed to build the response surface for the marginal distribution parameters of rainfall at every pixel.~~

The left panel of Fig. 7 provides the pointwise 10-year unconditional return level map over the case study area for 36 hr rainfall extremes. The value at the location of interest—the blue star (the centroid of Bellinger catchment)—is around 260 mm. The right panel of Fig. 7 indicates that when accounting for the effect of a 20-year event for 36 hr rainfall extremes happening at the location of the red star (the centroid of Kalang River catchment), the pointwise one in 10 chance conditional return level at the blue star rises to around 453 mm (i.e., 1.74 times the unconditional value).

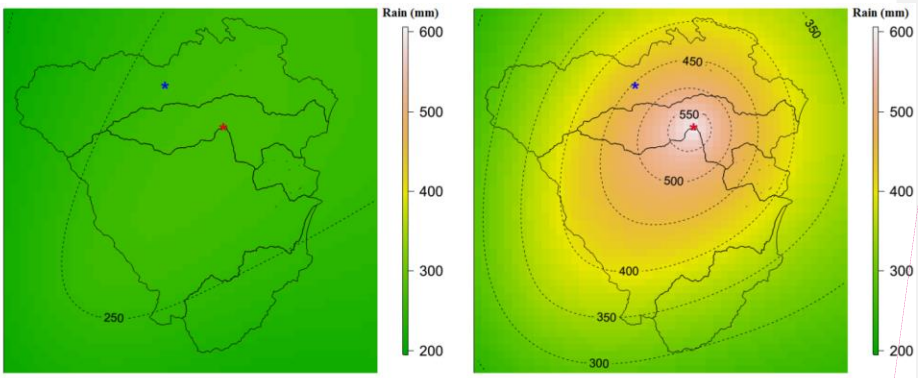


Formatted: English (United States)

**Figure 7.** Pointwise 10-year unconditional return level map (mm) for 36 hr extremes (left), and pointwise one in 10 chance conditional return level map (mm) for 36 hr extremes given a 20-year event for 36 hr extremes happen at location of the red star for the centroid of Kalang River catchment (right). The colour scales are the same for comparison.

Figure 8 provides similar plots to Fig. 7 for another pair of locations having different durations of rainfall extremes due to different times of concentration in each catchment. Here, the location of interest is the centroid of the Deep Creek catchment (the blue star in Fig. 8) and the conditional point is the centroid of the Kalang River catchment (the red star in Fig. 8). The pointwise 10-year unconditional and one in 10 chance conditional return levels at the location of the blue star are 134 mm and 194 mm, respectively. The relative difference between the conditional and unconditional return levels is only 1.45 times, compared with 1.74 times for the case in Fig. 7. This is because the pair of locations in Fig. 8 has a longer distance than those in Fig. 7, so that the dependence level is weaker. Moreover, the location pair in Fig. 8 was analysed for different durations (between 36 and 9 hr extremes), which has weaker dependence than the case of the equivalent durations in Fig. 7 (between 36 and 36 hr), based on Fig. 6.

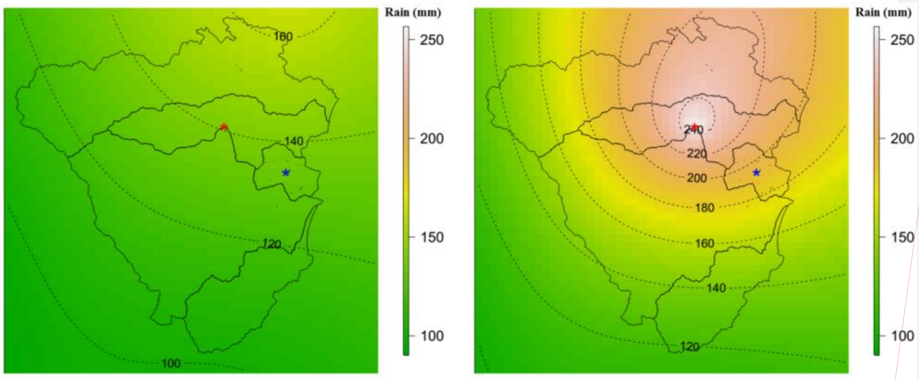


**Formatted:** English (United States)

**Figure 8.** Pointwise 10-year unconditional return level map (mm) for 9 hr extremes (left), and pointwise one in 10 chance conditional return level map (mm) for 9 hr extremes, given a 20-year event for 36 hr extremes happens at location of the red star for the centroid of the Kalang River catchment (right). The colour scales are the same for comparison.

~~The unconditional and conditional return levels are transformed to flood flows via the hydrological model WBNM previously calibrated to each catchment (WMAWater, 2011).~~ The unconditional and conditional return levels were extracted at the centroid of each main catchment, ~~which~~and were ~~then~~ converted to the ~~average spatial~~absolute values of rainfall using ~~an areal reduction factor (ARF). The~~a corresponding ARF and design storm hyetograph. The unconditional and conditional flood flows at the river crossing in the Bellinger catchment (corresponding to the unconditional and conditional rainfall extremes in Fig. 7) are given in Fig. 9 (left panel). Similar plots for the river crossing in the Deep Creek catchment (corresponding to the unconditional and conditional rainfall extremes in Fig. 8) are given in Fig. 9 (right panel).

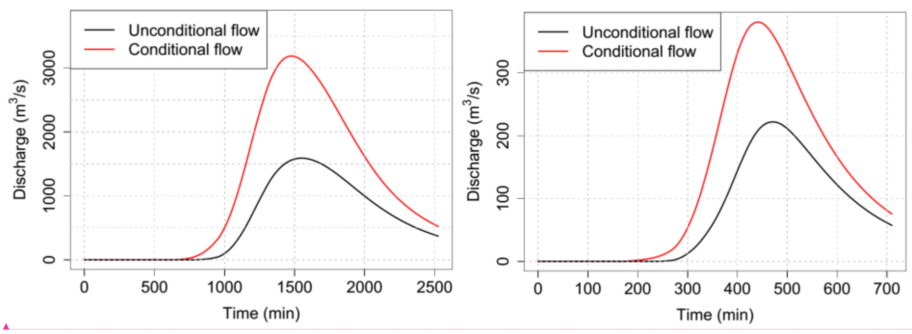


**Figure 9.** Comparison between conditional flows (red line) and unconditional flows (black line). (left) At the river crossing in the Bellinger catchment (number 1 in Figure 3): conditional flow caused by an one in 10 chance conditional event for 36 hr rainfall in considering the effect of a 20-year event for 36 hr rainfall occurring at the river crossing in the Kalang River catchment, and unconditional flow caused by a 10-year unconditional event for 36 hr. (right) At the river crossing in the Deep Creek catchment (number 3 in Figure 3): conditional flow caused by an one in 10 chance conditional event for 9 hr rainfall in considering the effect of a 20-year event for 36 hr rainfall occurring at the river crossing in the Kalang River catchment, and unconditional flow caused by a 10-year unconditional event for 9 hr rainfall.

Fig. ~~The~~ 9 presents peak flow for the Bellinger (left panel ~~of Fig. 9 indicates~~) and Deep Creek (right panel) catchments, indicating that the peak conditional flow at the river ~~crossing in the Bellinger catchment~~crossings is almost 2.0 and 1.7 times higher than ~~that for~~the unconditional flow~~. The time taken to reach to the peaks is the same~~ for ~~both cases. This is because this river crossing is affected by a large region with a long time of concentration (36 hr); the impact of rainfall losses on the hydrograph is insignificant.~~the two catchments, respectively. This difference is a direct result of the conditional ~~relationship being more stringent~~event having a higher rainfall magnitude than the unconditional

**Formatted:** English (United States)

~~relationship. Given~~event: given that there is an ~~existing~~ extreme event nearby, it is more likely for an extreme event to occur at ~~another~~a nearby location ~~of interest in the region~~. If a bridge design were to take into account this extra criterion for the purposes of evacuation planning it would require the design to be at a higher level.

~~Shown in the right panel in Fig. 9, the peak of the conditional flow at the river crossing in the Deep Creek catchment occurred earlier, and is around 1.7 times higher than that for the unconditional flow. This is due to the fact that the river crossing in Deep Creek covers a small region with a short time of concentration (9 hr) and the impact of rainfall losses on the hydrograph is significant. Although Fig. 9 shows a difference in terms of the time taken to reach the peak flows, the two design hydrographs are separate and this is not a physical timing difference.~~

### *5.3. Estimating the failure probability of the highway section based on the joint probability of rainfall extremes*

~~The recommended approach for estimating the overall failure probability of a system is demonstrated by considering a hypothetical traffic system with multiple river crossings at locations $x_1, \dots, x_N$. If there is a one-to-one correspondence between extreme rainfall intensity over a catchment and flood magnitude, the overall failure probability will be approximately equal to the probability that there is at least one river crossing whose contributing catchment has rainfall extremes exceeding the design level, which can be estimated using a large number of simulations from the spatial rainfall model. This approach is applied to the Pacific Highway upgrade project containing five river crossings. A set of 10,000 year simulated rainfall (Section 4.5) is generated from the fitted model (Section 5.1) to calculate the overall failure probability of the highway section. This process is repeated 100 times to estimate the average failure probability, under the assumption that all river crossings are designed to the same individual failure probability.~~

Figure 10 is a plot of the overall failure probability of the highway as a function of the failure probability of each individual river crossing (black). Similar relationships for the cases of complete dependence (blue) and ~~complete~~ independence (red) are also provided for comparison. For the case of complete dependence, when the whole region is extreme at the same time, the overall failure probability of the highway is equal to the individual river crossing failure probability and it represents the ~~best case (the~~ lowest overall failure probability~~).~~. The worst case is complete independence where extremes do not happen together unless by random chance; this means the failure probability of the highway is much higher than that for individual river crossings. Taking into account the real dependence, there are some extremes that align and it seems from ~~the~~ Fig. 10 that this is a relatively weak effect. As an example from Fig. 10, to design the highway with a failure probability of 1% ~~AEP,~~annual exceedance probability (AEP), we would have to design each individual river crossing to a much rarer AEP of 0.25% (see green lines in Fig. 10).

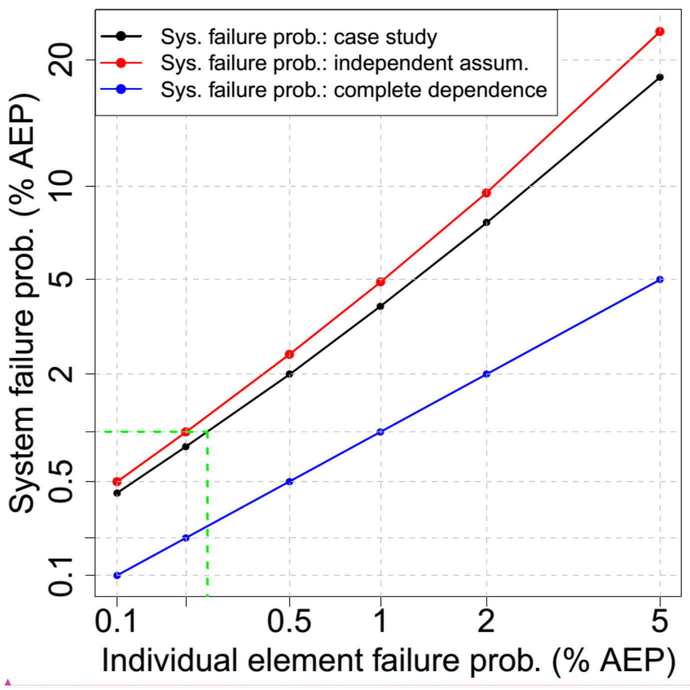


**Formatted:** English (United States)

**Figure 10.** Relationship between system failure probability and individual element failure probability in % annual exceedance probability (% AEP). The black colour is for the case study, the red colour is for the case of ~~complete~~ independence, and the blue colour is for the case of complete dependence. The green lines help to interpolate the individual

element failure probability from a given system failure probability of 1%. Both horizontal axis and vertical axis are constructed at a double log scale for viewing purposes.

## 6. Discussion and Conclusions

Hydrological design~~,~~ that is based on IDF ~~curves,~~estimates has conventionally focussed on ~~individual catchments and individual extremes.~~separate estimation at single locations. Such an approach can lead to ~~an underestimation~~the misspecification of wider system risk of flooding since weather systems exhibit dependence in space~~ and~~, time and across storm durations, which can lead to the coincidence of extremes. A number of methods have been developed to address the problem of antecedent moisture within a single catchment, by accounting for the temporal dependence of rainfall at locations of interest through loss parameters or sampling rainfall patterns ~~(Rahman et al., 2002)~~(Rahman et al., 2002). However, there have been fewer methods that account for the spatial dependence of rainfall across multiple catchments, due in part to the complexity of representing the effects of spatial dependence in risk calculations. Different catchments can have different times of concentration, so spatial dependence may also imply the need to consider dependence across different durations of extreme rainfall bursts.

Recent and ongoing advances in modelling spatial rainfall extremes provide an opportunity to revisit the scope of hydrological design. Such models include a max-stable model fitted using a Bayesian hierarchical approach ~~(Stephenson et al., 2016)~~(Stephenson et al., 2016), max-stable and inverted max-stable models ~~(Nicolet et al., 2017; Padoan et al., 2010; Russell et al., 2016; Thibaud et al., 2013; Westra and Sisson, 2011)~~(Nicolet et al., 2017; Padoan et al., 2010; Russell et al., 2016; Thibaud et al., 2013; Westra and Sisson, 2011) and latent-variable Gaussian models (Bennett et al., 2016b). The ability to simulate rainfall over a region means that hydrological problems need not be confined to individual catchments, but may cover multiple catchments. Civil infrastructure systems such as highways, railways or levees are such examples, since the failure of any one element may lead to overall failure of the system. Alternatively, where there is a network, the failure of one element may have implications for the overall system to accommodate the loss, by considering alternative routes. With models of spatial dependence and duration dependence of extremes, there is a new and improved ability to address these problems explicitly as part of the design methodology.

This paper demonstrated an application for evaluating conditional and joint probabilities of flood at different locations. This was achieved with two examples: (i) the design of a river crossing that will fail once on average every $M$ times given that its neighbouring river crossing is flooded; and (ii) estimating the probability that a highway section, which contains multiple river crossings, will fail based on the failure probability of each individual river crossing. Due to the lack of continuous streamflow data and ~~subdaily~~sub-daily limitations of rain-based continuous simulation, this study used an event-based method of conditional and joint rainfall extremes to estimate the corresponding conditional and joint flood flows. The spatial rainfall was simulated using an asymptotically independent model, which was then used to estimate conditional and joint rainfall extremes. An empirical method was obtained from the framework of ~~Le et al. (2018b)~~Le et al. (2018b) to make an asymptotically independent model—the inverted max-stable process—able to capture the spatial dependence of rainfall extremes across different durations. The fitted residual tail dependence coefficient function showed that the model can capture the dependence for different pairs of durations. For our example, the highest ratio of the one in 10 chance conditional event (in considering the effect of a 20-year event rainfall occurring at the conditional location) to the 10-year unconditional event was 1.74, for the two catchments having the strongest dependence (Fig. 7). The corresponding conditional flows were then estimated using a hydrological model WBNM and shown to be strongly related to the ratio of conditional and unconditional rainfall extremes (Fig. 9).

The joint probability of rainfall extremes for all catchments and for all possible pairs of catchments in the case study area was estimated empirically from a set of 10,000 years of simulated rainfall extremes, repeated 100 times to estimate the average value. The results showed that there were differences in the failure probability of the highway after taking into account the rainfall dependence, but the effect was not as emphatic as with the case of conditional probabilities. The difference in the failure probability became weaker as the return period increased, which is consistent with the characteristic of asymptotically independent data ~~(Ledford and Tawn, 1996; Wadsworth and Tawn, 2012)~~(Ledford and Tawn, 1996; Wadsworth and Tawn, 2012). A relationship was demonstrated (Fig. 10) to show how the design of the overall system to a given failure probability requires the design of each individual river crossing to a rarer extremal level than when each crossing is considered in isolation. For the case study example, it would be necessary to design each ~~bridge~~of the five bridges to a 0.25% AEP event in order to obtain a system failure probability of 1%.

There is a need to reimagine the role of intensity-duration-frequency ~~curves.~~relationships. Conventionally they have been developed as maps of the marginal rainfall in a point-wise manner for all locations and for a range of frequencies and durations. The increasing sophistication of mathematical models for extremes, computational power and interactive graphics abilities of online mapping platforms means that analysis of hydrological extremes could significantly expand in scope. With an underlying model of spatial and duration dependence between the extremes, it is not difficult to conceive of digital maps that dynamically transform from the marginal representation of extremes to the corresponding representation conditional extremes after any number of conditions are applied. This transformation is exemplified by the differences between left and right panels in Fig. 7 and Fig. 8. Enhanced IDF maps would enable a very different paradigm of design flood risk estimation, breaking away from analysing individual system elements in isolation ~~to emphasize~~and instead emphasizing the behaviour of entire system.

## Appendix A. Calculation of empirical tail dependence coefficient

To illustrate how Eq. (~~4~~2) in the manuscript is calculated, consider a set of $n = 10$ observed values at the two locations: $Z_1$ and $Z_2$ (see Table A1). First, $Z_1$ and $Z_2$ are converted to empirical cumulative probability estimates via the Weibull plotting position formula $P = j/(n+1)$ where $j$ is ranked index of a data point giving $P_1$ and $P_2$ (see Table A1).

**Table A1.** Observed data $Z_1$ and $Z_2$ and corresponding empirical cumulative probabilities $P_1$ and $P_2$.

| $Z_1$ | $Z_2$ | $P_1$ | $P_2$ |
|---|---|---|---|
| 5 | 10 | 0.455 | 0.909 |
| 9 | 1 | 0.818 | 0.091 |
| 1 | 7 | 0.091 | 0.636 |
| 2 | 6 | 0.182 | 0.545 |
| 10 | 4 | 0.909 | 0.364 |
| 3 | 3 | 0.273 | 0.273 |
| 8 | 9 | 0.727 | 0.818 |
| 6 | 2 | 0.545 | 0.182 |
| 4 | 8 | 0.364 | 0.727 |
| 7 | 5 | 0.636 | 0.455 |

Formatted Table

Assume that interest is in values above a threshold $u$ ~~=~~ satisfying $P_u = 0.5$, in other words, $P\cancel{\{Z_2 > z\}}\{Z_2 > u\} = P\cancel{\{P_2 > u\} =}\{P_2 > P_u\} = 0.5$. In this case we have only one pair, at the index of 7, that satisfy both $P_1$ and $P_2$ are greater than $\cancel{u =} P_u = 0.5$, thus $P\cancel{\{Z_1 > z, Z_2 > z\}}\{Z_1 > u, Z_2 > u\} = P\cancel{\{P_1 > u, P_2 > u\} = 1/10}\{P_1 > P_u, P_2 > P_u\} = 1/10 = 0.1$. The calculation of the empirical tail dependence coefficient is then

$$\eta(x_1, x_2) = \cancel{\frac{\log P\{Z_2 > z\}}{\log P\{Z_1 > z, Z_2 > z\}} = \frac{\log P\{P_2 > u\}}{\log P\{P_1 > u, P_2 > u\}} = \frac{\log(0.5)}{\log(0.1)}} \frac{\log P\{Z_2 > u\}}{\log P\{Z_1 > u, Z_2 > u\}}$$

$$= \frac{\log P\{P_2 > P_u\}}{\log P\{P_1 > P_u, P_2 > P_u\}} = \frac{\log(0.5)}{\log(0.1)} = 0.301. \qquad (A.1)$$

## *Appendix B Estimate of conditional and joint probabilities of rainfall extremes*

The unit Fréchet transformation is given as

$$z = \begin{cases} \left(log\left\{1 - \Phi_u\left(1 + \frac{\xi(y-u)}{\sigma_u}\right)^{-1/\xi}\right\}\right)^{-1} & y > u, \xi \neq 0 \\ -\left(log\left\{1 - \Phi_u exp\left(-\frac{y-u}{\sigma_u}\right)^{-1/\xi}\right\}\right)^{-1} & y > u, \xi = 0 \\ -\{logF(y_i)\}^{-1} & y \leq u \end{cases} \qquad (B.1)$$

where $y$ is the original marginal value and $z$ is the Fréchet transformed value and all other parameters correspond to the GPD specified in Section 4.1. For values below the threshold, $F$ is the empirical distribution function of $y$, $F(y_i) = i/(n+1)$ where $i$ is the rank of $y_i$ and $n$ is the total number of data points.

The conditional probability $P\{Z_2 > z_2 | Z_1 > z_1\}$ is obtained from the bivariate inverted max-stable process cumulative distribution function (CDF) in unit Fréchet margins (Thibaud et al., 2013), which is given as:

$$P\{Z_1 \leq z_1, Z_2 \leq z_2\} = 1 - \exp\left\{-\frac{1}{g_1}\right\} - \exp\left\{-\frac{1}{g_2}\right\} + \exp[-V\{g_1, g_2\}], \qquad (B.2)$$

where $g_1 = -1/\log\{1 - \exp(-1/z_1)\}$, $g_2 = -1/\log\{1 - \exp(-1/z_2)\}$, and the exponent measure $V$ (Padoan et al., 2010) is defined as:

$$V\{g_1, g_2\} = -\frac{1}{g_1}\Phi\left\{\frac{a}{2} + \frac{1}{a}log\frac{g_2}{g_1}\right\} - \frac{1}{g_2}\Phi\left\{\frac{a}{2} + \frac{1}{a}log\frac{g_1}{g_2}\right\}. \qquad (B.3)$$

In Eq. (B.3), $\Phi$ is the standard normal cumulative distribution function, $a = \sqrt{2\gamma_{ad.}(h)}$ with $\gamma_{ad.}(h)$ is the variograms that was mentioned in the explanation of Eq. (3).

In unit Fréchet margins, the relationship between the return level $z$ and the return period $T$ (in number of observations) is given as $z = -1/log(1 - 1/T)$, and the conditional probability for the max-stable process can then be estimated using:

$$P\{Z_2 > z_2 | Z_1 > z_1\} = T_1\left[\frac{1}{T_1} - \exp\left(-\frac{1}{z_2}\right) + P\{Z_1 \leq z_1, Z_2 \leq z_2\}\right], \qquad (B.4)$$

where $T_1$ is the return period (in number of observations for 36 hr rainfall) corresponding to the return level $z_1$. It is also noted that in this paper $Z_1$ and $Z_2$ were taken as threshold exceedances, so the return period $T_1$ should be in the number of observations, which is equivalent to a $T_1/243$–year return period because there are 243 observations for 36 hr rainfall in a year.

The probability that there is at least one location that has an extreme event exceeding a given threshold can be calculated based on the addition rule for the union of probabilities, as:

$$P(Z_1 > z_1 \text{ or} \dots \text{or } Z_N > z_N) = \sum_{i=1}^{N} P(Z_i > z_i) - \sum_{i<j} P\big(Z_i > z_i, Z_j > z_j\big) + \cdots$$

$$+(-1)^{N-1} P(Z_1 > z_1, \dots, Z_N > z_N), \qquad (B.5)$$

where $N$ is the number of locations.

For the case of dependent variables, the joint probability for only two locations $P\{Z_1 > z_1, Z_2 > z_2\}$ can be easily obtained from the bivariate CDF for inverted max-stable process in Eq. (B.2). However, for the case of multiple locations (five different locations for this paper), it is difficult to derive the formula for this probability because there are dependences between extreme events at all locations. So this probability is empirically calculated from a large number of simulations of the dependent model (see the description of the simulation procedure for an inverted max-stable process in Section 4.3).

For the case that all of events are independent, the joint probability for independent variables is broken down as the product of the marginals, and the conditional probability is equivalent to the marginal probability. When applying Eq. (B.5) for independent variables, the joint probability is therefore calculated by $P(Z_1 > z_1, \dots, Z_N > z_N) = P(Z_1 > z_1) \dots P(Z_N > z_N)$.

**Acknowledgments**

The lead author was supported by the Australia Awards Scholarships (AAS) from Australia Government. A/Prof Westra was supported by Australian Research Council Discovery grant DP150100411. We thank Mark Babister and Isabelle Testoni of WMA Water for providing the hydrologic models for the case study; and Leticia Mooney for her editorial help in improving this

manuscript. The rainfall data used in this study were provided by the Australian Bureau of Meteorology, and can be obtained from the corresponding author.

## References


Asadi, P., Davison, A. C., and Engelke, S.: Extremes on river networks, Ann. Appl. Stat., 9, 2023-2050, 10.1214/15-AOAS863, 2015.

Ball, J., Babister, M., Nathan, R., Weeks, W., Weinmann, E., Retallick, M., and Testoni, I.: Australian Rainfall and Runoff: A Guide to Flood Estimation, © Commonwealth of Australia (Geoscience Australia), 2016.

Bárdossy, A., and Pegram, G. G. S.: Copula based multisite model for daily precipitation simulation, Hydrol. Earth Syst. Sci., 13, 2299-2314, 10.5194/hess-13-2299-2009, 2009.

Baxevani, A., and Lennartsson, J.: A spatiotemporal precipitation generator based on a censored latent Gaussian field, Water Resources Research, 51, 4338-4358, doi:10.1002/2014WR016455, 2015.

Bennett, B., Lambert, M., Thyer, M., Bates, B. C., and Leonard, M.: Estimating Extreme Spatial Rainfall Intensities, Journal of Hydrologic Engineering, 21, 04015074, doi:10.1061/(ASCE)HE.1943-5584.0001316, 2016a.

Bennett, B., Thyer, M., Leonard, M., Lambert, M., and Bates, B.: A comprehensive and systematic evaluation framework for a parsimonious daily rainfall field model, Journal of Hydrology, https://doi.org/10.1016/j.jhydrol.2016.12.043, 2016b.

Bernard, M. M.: Formulas for rainfall intensities of long duration, Transactions of the American Society of Civil Engineers, 96, 592-606, 1932.

Boughton, W., and Droop, O.: Continuous simulation for design flood estimation—a review, Environmental Modelling & Software, 18, 309-318, https://doi.org/10.1016/S1364-8152(03)00004-5, 2003.

Boyd, M. J., Rigby, E. H., and VanDrie, R.: WBNM — a computer software package for flood hydrograph studies, Environmental Software, 11, 167-172, https://doi.org/10.1016/S0266-9838(96)00042-1, 1996.

Brown, B. M., and Resnick, S. I.: Extreme Values of Independent Stochastic Processes, Journal of Applied Probability, 14, 732-739, 10.2307/3213346, 1977.

Cameron, D. S., Beven, K. J., Tawn, J., Blazkova, S., and Naden, P.: Flood frequency estimation by continuous simulation for a gauged upland catchment (with uncertainty), Journal of Hydrology, 219, 169-187, https://doi.org/10.1016/S0022-1694(99)00057-8, 1999.

Carreau, J., Neppel, L., Arnaud, P., and Cantet, P.: Extreme Rainfall Analysis at Ungaug ed Sites in the South of France : Comparison of Three Approaches, Jour nal de la Société Française de Statistique, 154 No. 2, 119-138, 2013.

Chow, V. T., Maidment, D. R., and Mays, L. W.: Applied Hydrology, McGraw-Hill, c1988, New York, 1988.

Coles, S., Heffernan, J., and Tawn, J.: Dependence Measures for Extreme Value Analyses, Extremes, 2, 339-365, 10.1023/a:1009963131610, 1999.

Coles, S.: An Introduction to Statistical Modeling of Extreme Values, Springer Series in Statistics, Springer, 2001.

Davison, A. C., and Smith, R. L.: Models for exceedances over high thresholds, Journal of the Royal Statistical Society. Series B (Methodological), 393-442, 1990.

Davison, A. C., Padoan, S. A., and Ribatet, M.: Statistical Modeling of Spatial Extremes, Statistical Science, 161-186, 10.1214/11-STS376, 2012.

de Haan, L.: A Spectral Representation for Max-stable Processes, The Annals of Probability, 12, 1194-1204, 10.2307/2243357, 1984.

Demarta, S., and McNeil, A. J.: The t Copula and Related Copulas, International Statistical Review / Revue Internationale de Statistique, 73, 111-129, 2005.

Dombry, C., Engelke, S., and Oesting, M.: Exact simulation of max-stable processes, Biometrika, 103, 303-317, 2016.

Durocher, M., Chebana, F., and Ouarda, T. B. M. J.: On the prediction of extreme flood quantiles at ungauged locations with spatial copula, Journal of Hydrology, 533, 523-532, https://doi.org/10.1016/j.jhydrol.2015.12.029, 2016.

Favre, A. C., Adlouni, S. E., Perreault, L., Thiémonge, N., and Bobée, B.: Multivariate hydrological frequency analysis using copulas, Water Resources Research, 40, doi:10.1029/2003WR002456, 2004.

Gupta, A. S., and Tarboton, D. G.: A tool for downscaling weather data from large-grid reanalysis products to finer spatial scales for distributed hydrological applications, Environmental Modelling & Software, 84, 50-69, https://doi.org/10.1016/j.envsoft.2016.06.014, 2016.

He, Y., Bárdossy, A., and Zehe, E.: A review of regionalisation for continuous streamflow simulation, Hydrology and Earth System Sciences, 15, 3539, 2011.

Hegnauer, M., Beersma, J., Van den Boogaard, H., Buishand, T., and Passchier, R.: Generator of Rainfall and Discharge Extremes (GRADE) for the Rhine and Meuse basins; Final report of GRADE 2.0, Document extern project, 2014.

Hosking, J. R. M., and Wallis, J. R.: Regional Frequency Analysis - An Approach Based on L-Moments, Cambridge University Press, Cambridge, UK, 1997.

Huser, R., and Davison, A. C.: Composite likelihood estimation for the Brown–Resnick process, Biometrika, 100, 511-518, 10.1093/biomet/ass089, 2013.

Hüsler, J., and Reiss, R.-D.: Maxima of normal random vectors: Between independence and complete dependence, Statistics & Probability Letters, 7, 283-286, https://doi.org/10.1016/0167-7152(89)90106-5, 1989.

Kabluchko, Z., Schlather, M., and de Haan, L.: Stationary Max-Stable Fields Associated to Negative Definite Functions, The Annals of Probability, 37, 2042-2065, 2009.

Kao, S.-C., and Govindaraju, R. S.: Trivariate statistical analysis of extreme rainfall events via the Plackett family of copulas, Water Resources Research, 44, doi:10.1029/2007WR006261, 2008.

Kleiber, W., Katz, R. W., and Rajagopalan, B.: Daily spatiotemporal precipitation simulation using latent and transformed Gaussian processes, Water Resources Research, 48, doi:10.1029/2011WR011105, 2012.

Koutsoyiannis, D., Kozonis, D., and Manetas, A.: A mathematical framework for studying rainfall intensity-duration-frequency relationships, Journal of Hydrology, 206, 118-135, http://dx.doi.org/10.1016/S0022-1694(98)00097-3, 1998.

Kuichling, E.: The relation between the rainfall and the discharge of sewers in populous districts, Transactions of the American Society of Civil Engineers, 20, 1-56, 1889.

Laurenson, E. M., and Mein, R. G.: RORB Version 4 Runoff Routing Program User Manual, Monash University Department of Civil Engineering, 1997.

Le, P. D., Davison, A. C., Engelke, S., Leonard, M., and Westra, S.: Dependence properties of spatial rainfall extremes and areal reduction factors, Journal of Hydrology, 565, 711-719, https://doi.org/10.1016/j.jhydrol.2018.08.061, 2018a.

Le, P. D., Leonard, M., and Westra, S.: Modeling Spatial Dependence of Rainfall Extremes Across Multiple Durations, Water Resources Research, 54, 2233-2248, doi:10.1002/2017WR022231, 2018b.

Ledford, A. W., and Tawn, J. A.: Statistics for Near Independence in Multivariate Extreme Values, Biometrika, 83, 169-187, 1996.

Leonard, M., Lambert, M. F., Metcalfe, A. V., and Cowpertwait, P. S. P.: A space-time Neyman–Scott rainfall model with defined storm extent, Water Resources Research, 44, doi:10.1029/2007WR006110, 2008.

Leonard, M., Westra, S., Phatak, A., Lambert, M., Hurk, B. v. d., McInnes, K., Risbey, J., Schuster, S., Jakob, D., and Stafford-Smith, M.: A compound event framework for understanding extreme impacts, Wiley Interdisciplinary Reviews: Climate Change, 5, 113-128, doi:10.1002/wcc.252, 2014.

Mulvaney, T. J.: On the use of self-registering rain and flood gauges in making observation of the relation of rainfall and floods discharges in a given catchment, Proc. Civ. Eng. Ireland, 4, 18–31, 1851.

Nicolet, G., Eckert, N., Morin, S., and Blanchet, J.: A multi-criteria leave-two-out cross-validation procedure for max-stable process selection, Spatial Statistics, 22, 107-128, https://doi.org/10.1016/j.spasta.2017.09.004, 2017.

Oesting, M., Schlather, M., and Friederichs, P.: Statistical post-processing of forecasts for extremes using bivariate Brown-Resnick processes with an application to wind gusts, Extremes, 20, 309-332, 10.1007/s10687-016-0277-x, 2017.

Opitz, T.: Extremal t processes: Elliptical domain of attraction and a spectral representation, Journal of Multivariate Analysis, 122, 409-413, https://doi.org/10.1016/j.jmva.2013.08.008, 2013.

Padoan, S. A., Ribatet, M., and Sisson, S. A.: Likelihood-Based Inference for Max-Stable Processes, Journal of the American Statistical Association, 105, 263-277, 10.1198/jasa.2009.tm08577, 2010.

Pathiraja, S., Westra, S., and Sharma, A.: Why continuous simulation? The role of antecedent moisture in design flood estimation, Water Resources Research, 48, doi:10.1029/2011WR010997, 2012.

Pickands, J.: Statistical Inference Using Extreme Order Statistics, The Annals of Statistics, 3, 119-131, 10.2307/2958083, 1975.

Rahman, A., Weinmann, P. E., Hoang, T. M. T., and Laurenson, E. M.: Monte Carlo simulation of flood frequency curves from rainfall, Journal of Hydrology, 256, 196-210, https://doi.org/10.1016/S0022-1694(01)00533-9, 2002.

Rasmussen, P. F.: Multisite precipitation generation using a latent autoregressive model, Water Resources Research, 49, 1845-1857, doi:10.1002/wrcr.20164, 2013.

Renard, B., and Lang, M.: Use of a Gaussian copula for multivariate extreme value analysis: Some case studies in hydrology, Advances in Water Resources, 30, 897-912, http://dx.doi.org/10.1016/j.advwatres.2006.08.001, 2007.

Requena, A. I., Chebana, F., and Ouarda, T. B. M. J.: A functional framework for flow-duration-curve and daily streamflow estimation at ungauged sites, Advances in Water Resources, 113, 328-340, https://doi.org/10.1016/j.advwatres.2018.01.019, 2018.

Russell, B. T., Cooley, D. S., Porter, W. C., and Heald, C. L.: Modeling the spatial behavior of the meteorological drivers' effects on extreme ozone, Environmetrics, 27, 334-344, doi:10.1002/env.2406, 2016.

Schlather, M.: Models for Stationary Max-Stable Random Fields, Extremes, 5, 33-44, 10.1023/A:1020977924878, 2002.

Seneviratne, S. I., Nicholls, N., Easterling, D., Goodess, C. M., Kanae, S., Kossin, J., Luo, Y., Marengo, J., McInnes, K., and Rahimi, M.: Managing the Risks of Extreme Events and Disasters to Advance Climate Change Adaptation: Changes in Climate Extremes and their Impacts on the Natural Physical Environment, 2012.

Nambucca Heads Flood Study: http://www.nambucca.nsw.gov.au/cp_content/resources/16152_2011__Nambucca_Heads_Flood_Study_Final_Draft_Chapter_6a.pdf, 2011.

Stedinger, J., Vogel, R., and Foufoula-Georgiou, E.: Frequency Analysis of Extreme Events, in: Handbook of Hydrology, edited by: Maidment, D. R., McGraw-Hill, New York, 18.11-18.66, 1993.

Stephenson, A. G., Lehmann, E. A., and Phatak, A.: A max-stable process model for rainfall extremes at different accumulation durations, Weather and Climate Extremes, 13, 44-53, https://doi.org/10.1016/j.wace.2016.07.002, 2016.

Thibaud, E., Mutzner, R., and Davison, A. C.: Threshold modeling of extreme spatial rainfall, Water Resources Research, 49, 4633-4644, 10.1002/wrcr.20329, 2013.

Wadsworth, J. L., and Tawn, J. A.: Dependence modelling for spatial extremes, Biometrika, 99, 253-272, 10.1093/biomet/asr080, 2012.

Wang, Q. J.: A Bayesian Joint Probability Approach for flood record augmentation, Water Resources Research, 37, 1707-1712, 10.1029/2000WR900401, 2001.

Wang, Q. J., Robertson, D. E., and Chiew, F. H. S.: A Bayesian joint probability modeling approach for seasonal forecasting of streamflows at multiple sites, Water Resources Research, 45, doi:10.1029/2008WR007355, 2009.

Wang, X., Gebremichael, M., and Yan, J.: Weighted likelihood copula modeling of extreme rainfall events in Connecticut, Journal of Hydrology, 390, 108-115, http://dx.doi.org/10.1016/j.jhydrol.2010.06.039, 2010.

Westra, S., and Sisson, S. A.: Detection of non-stationarity in precipitation extremes using a max-stable process model, Journal of Hydrology, 406, 119-128, http://dx.doi.org/10.1016/j.jhydrol.2011.06.014, 2011.

WMAWater: Review of Bellinger, Kalang and Nambucca River Catchments Hydrology, Bellingen Shire Council, Nambucca Shire Council, New South Wales Government, 2011.

Zhang, L., and Singh, V. P.: Gumbel–Hougaard Copula for Trivariate Rainfall Frequency Analysis, Journal of Hydrologic Engineering, 12, 409-419, doi:10.1061/(ASCE)1084-0699(2007)12:4(409), 2007.

Zheng, F., Westra, S., and Leonard, M.: Opposing local precipitation extremes, Nature Clim. Change, 5, 389-390, 10.1038/nclimate2579 http://www.nature.com/nclimate/journal/v5/n5/abs/nclimate2579.html#supplementary-information, 2015.

Zscheischler, J., Westra, S., van den Hurk, B. J. J. M., Seneviratne, S. I., Ward, P. J., Pitman, A., AghaKouchak, A., Bresch, D. N., Leonard, M., Wahl, T., and Zhang, X.: Future climate risk from compound events, Nature Climate Change, 8, 469-477, 10.1038/s41558-018-0156-3, 2018.